Climate Modelling User Group

Deliverable 3.1

Quality Assessment Report

Centres providing input: Met Office, MPI-M, ECMWF, MétéoFrance, IPSL, BSC

Revision nr.	Date	Status
0.1	26 July 2019	Agreed outline and scope of content with ESA
0.2	9 Sept. 2019	First input from partners of activity and results, Met Office, IPSL, BSC
1.0	24 Sept 2019	Input from all WP3 partners, submission to ESA
1.1	21 Feb 2020	Address comments from ESA
1.2	March 2020	Accepted by ESA
1.3	August 2020	Typo corrected
2.0	20 Sept 2021	Update from all WP3 partners, submission to ESA
2.1	01 Nov 2021	Responded to RID_v2 resubmit to ESA

CMUG CCI+ Deliverable 3.1

Quality Assessment Report

Table of Contents

Technical report on quality assessment

1. Purpose and scope of this report

This document is the second technical report on the Quality Assessment of CCI ECVs in the CCI+ phase of the initiative. Its purpose is to assess the quality of the available versions of CCI products and update feedback to ESA and the CCI teams. This assessment is being conducted by the climate modelling and reanalysis centres in the CMUG consortium using CCI Phase 2 and CCI+ Phase 1 data and includes a wide range of data and model interactions (assimilation, boundary conditions, optimisation, reanalysis, sensitivity studies etc.). This evaluation continues to examine the following top level questions:

- Are the CCI data products of 'climate quality' i.e. is their quality adequate for use in climate modelling, reanalysis and for wider research applications?
- Are the error characteristics provided by CCI products adequate?
- Do the products meet the Global Climate Observing System (GCOS) quality requirements for satellite for Essential Climate Variables (ECV)?
- Is the quality of the products sufficient for climate service applications?

2. CMUG approach for assessing quality in CCI products

This report describes the results in the second year of CMUG CCI+ Task 3 "Assessing consistency and quality of CCI products". The work is spread across twelve Work Packages (WP) listed in Table 1, which includes the CCI products being assessed, and the type of climate modelling experiment.

The CMUG results presented here provide information on the accuracy, consistency and usefulness of the CCI data sets available to CMUG up to July 2021. The analysis assesses the suitability of the CCI datasets for coupled climate model and reanalysis applications and evaluates the impact of the data products on model based studies, including quantification of the uncertainties associated with both the models and the observations. This information is aimed at the CCI teams producing the data but is also of use to other modelling centres which will use CCI data in the future.

CMUG WP 3: Quality Assessment of CCI products		Lead	Experiment type	CCI ECVs	Other ECVs
3.1	Consistency between CCI LST, SM product and LAI products	Météo France	Reanalysis, benchmarking	LST, SM	C3S LAI
3.2	Consistency between CCI Snow, SM product and LAI products	Météo France	Reanalysis, benchmarking	Snow, SM	C3S LAI
3.3	Consistency between CCI SM, PERMAFROST, and LAI products	Météo France	Reanalysis, benchmarking	Permafrost, SM	C3S LAI
3.4	Propagation of CCI(+) observational uncertainties to climate models scales	BSC	Statistical analysis	SM, Fire, LST	
3.5	Document SM-atmosphere feedbacks in transition regions (temperature and precipitation)	IPSL	Process analysis	SM, LST	turbulent fluxes, radiation, air temp, precip.
3.6	Better constrain evapotranspiration at the scale of climate model	IPSL	Process analysis	SM, Snow, LST	LAI, flux, radiation, air temp
3.7	The effect of Lakes on local temperatures	Met Office	Assimilation, process understanding	Lakes, LST	Lake surface temp datasets
3.8	Evaluation of the impact of an enhanced ESA Sea Ice reanalysis (EnESA-SIR) on initialization of seasonal prediction	BSC	Hindcast	SI thickness, concentration; salinity, SST	
3.9	Biophysical feedbacks in the global ocean	Met Office	Assimilation, reanalyses, process study	OC, SST, SI, Sea level, Salinity	Temp, salinity, carbon dioxide, ocean heat content
3.10	CCI/CCI+ data to constrain mineral dust simulations	BSC	Assimilation, stat. analysis	Aerosol dust, HRLC/LC	
3.11	Dust reanalysis at the regional scale	BSC	Assimilation, stat. analysis	Aerosol dust, HRLC/LC	
3.12	Integrated assimilation of the CCI+ Sentinel 3 AOD and Sentinel 5P ozone retrievals in the IFS	ECMWF	Reanalysis	Aerosol and Ozone	

Table 1: Main features of CMUG WP3 on assessing consistency and quality of CCI products across ECVs.

The modelling experiments are described in the following sections of this report and cover the following topics: assimilation of CCI data into climate models; cross assessments of CCI data (those which have physical links/interactions); benchmarking of models against observations; applications for reanalysis; statistical analysis; hindcasting; and Earth system process studies. The CMUG work reported here was conducted with the CCI data available at the time, which is the final Phase 2 Climate Record Data Packages produced by the CCI projects. Where the results are not yet available, the section is marked accordingly. A planned update of this report in the Summer of 2022 will include assessments missing from this version.

3. CMUG Quality Assessment Results

3.1 Consistency between CCI LST, and SM products

Lead partner: Météo-France
Author: Jean-Christophe Calvet

Aim

The aim of this research is to assess the consistency between CCI LST and SM products. It will address the following scientific questions:

1. How can land ECVs' consistency can be verified?
2. Are land ECVs represented well in climate and land surface models?
3. Can EO data improve land reanalyses?
4. Can EO data improve representation of extreme events (e.g. droughts)?

Summary of Work

The latest version of the CCI MODIS LST products was downloaded in May 2021.

Publications

None so far, but the interest in the results leading to a journal or conference publication will be described in the next version of this report.

Interactions with the ECVs used in this experiment

In the first 12 months of this phase of CMUG work there have been interactions with the SM and LST CCI ECV teams at the quarterly CSWG meetings and the Integration meetings. Contact outside that has been only to check on the continuation of the SM project, and to learn about the beta data that LST released in late 2019. Discussions with the LST-CCI team led to choosing the CCI MODIS LST products.

Consistency between data products

This section will provide a record of any inconsistencies found between ECV products, and will be completed in the next version of this report.

Recommendations to the CCI ECV teams

To be completed in next version of this report.

Plan for Year 3

This experiment is dependent on CCI LST data and now that a beta dataset is available the work can start. However, contrary to other ECV products, the LST-CCI portfolio contains many independent products instead of a single merged CDR. Integrating all of them in our application would be difficult. It must be noted that a number of independent products are already available to CMUG but that they are still under validation by the LST team. We will concentrate on the CCI MODIS LST products, covering the 2008-2018 time period.

3.2 Consistency between CCI Snow and SM products

Lead partner: Météo-France
Author: Jean-Christophe Calvet

Aim

The aim of this research is to assess the consistency between CCI Snow and SM products. It will address the following scientific questions:

1. How can land ECVs' consistency can be verified?
2. Are land ECVs represented well in climate and land surface models?
3. Can EO data improve land reanalyses?
4. Can EO data improve representation of extreme events (e.g. droughts)?

Summary of Work

The CCI SWE (Snow Water Equivalent) V1.1 product was assimilated in the ISBA land surface model using the LDAS-Monde tool; coupled with the CTRIP river discharge model. The experiment was conducted over Europe over the 2008-2018 time period. It was shown that the assimilation efficiently reduced the difference between SWE simulations and observations. Assimilating the CCI SWE improved the consistency between the simulated snow cover fraction (SCF) and the independent NOAA IMS SCF product. On the other hand, assimilating SWE had very little impact on the comparison between the simulated surface soil moisture (SM) and CCI SM. A hydrovalidation experiment was performed. It was based on the capability of LDAS-Monde to simulate river discharge. The comparison between simulated river discharge and in situ observations of river discharge showed that the assimilation of SWE tended to improve the simulations. The improvement was particularly large over the stations located in the Elbe river basin.

A more detailed report on the work carried out for this sub-work package will be included in the final version 3 of this document.

Publications

None so far, but the interest in the results leading to a journal or conference publication will be described in the next version of this report.

Interactions with the ECVs used in this experiment

The snow-permafrost cross-cutting evaluation was presented at the May 2021 CSWG session and at the May 2021 Snow-CCI user workshop.

Consistency between data products

Figure 3.2.1 shows that assimilating SWE has virtually no impact on the comparison between open-loop or analysed surface soil moisture with the SM-CCI product. However, a slight improvement can be observed over Scandinavia (NW region).

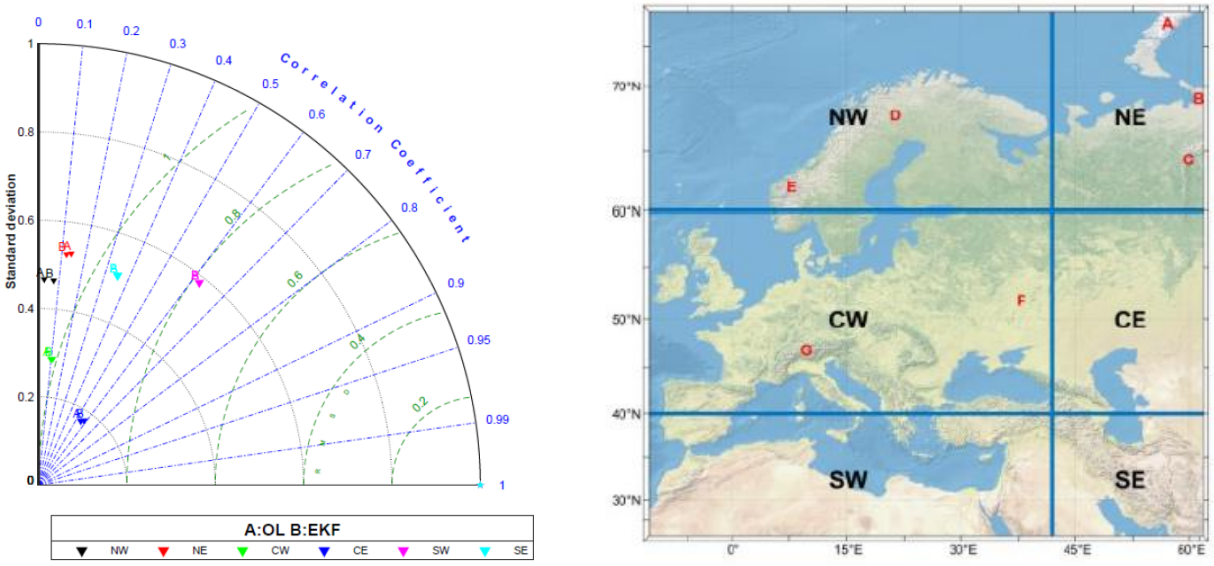

Figure 3.2.1*: Taylor diagram comparing open-loop (OL) and analyses (EKF) of a SWE assimilation experiment in terms of surface soil moisture score. The SM-CCI V5.2 dataset is used for the comparison. Six regions are considered (right panel): NW, NE, CW, CE, SW, SE.*

Figures 3.2.2 and 3.2.3 show that assimilating SWE has a positive impact on the simulated river discharge. The impact is particularly large over the Elbe river basin.

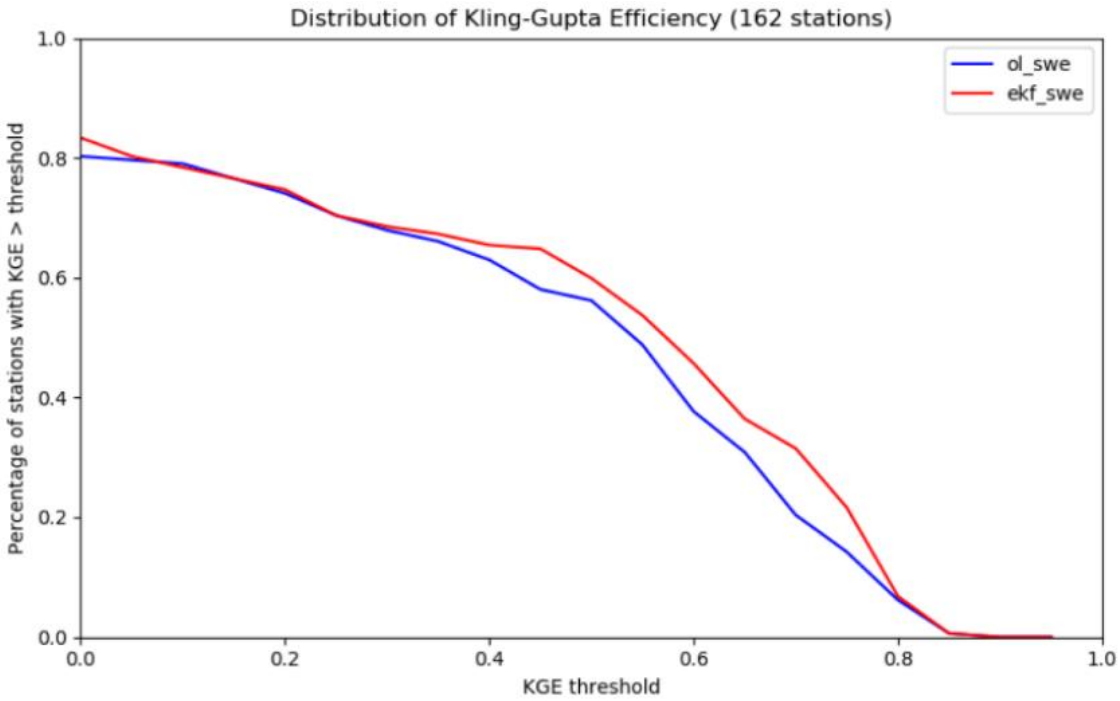

Figure 3.2.2*: Cumulative statistical distribution function of the Kling-Gupta Efficiency score of river discharge using the open-loop simulation (blue line) and the analysis resulting from the assimilation of the SWE product (red).*

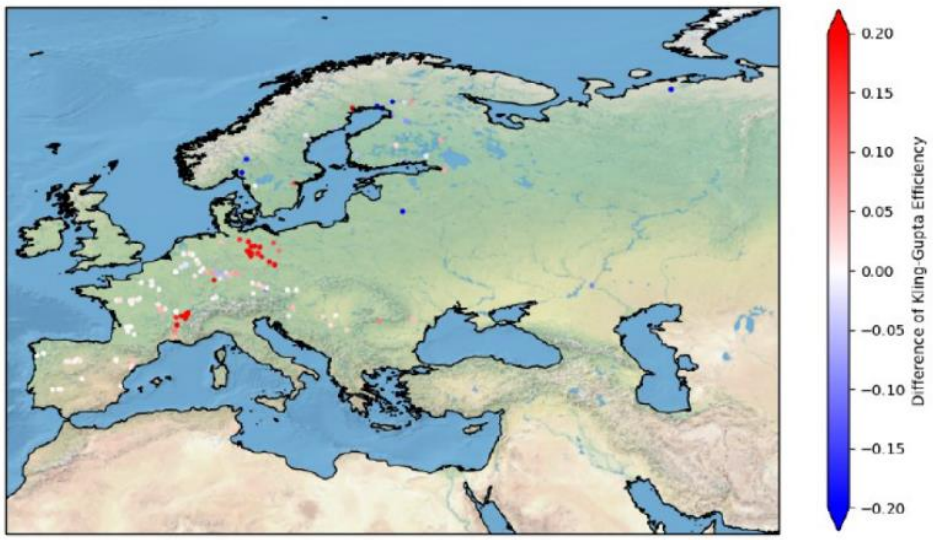

Figure 3.2.3: *Impact of assimilating SWE on the Kling-Gupta Efficiency score of river discharge over Europe.*

Recommendations to the CCI ECV teams

To be completed in next version of this report.

Plan for Year 3

To use the CCI Snow Cover Fraction product.

3.3 Consistency between CCI SM and PERMAFROST products

Lead partner: Météo-France
Author: Jean-Christophe Calvet

Aim

The aim of this research is to assess the consistency between CCI SM and CCI Permafrost products. It is noted that the CCI Permafrost data will be produced in a permafrost model forced with CCI SM data (amongst other data inputs) thus comparisons will be made with and without CCI SM. It will address the following scientific questions:

1. How can land ECVs consistency can be verified?
2. Are land ECVs represented well in climate and land surface models?
3. Can EO data improve land reanalyses?
4. Can EO data improve representation of extreme events (e.g. droughts)?

Summary of Work

The CCI SWE V1.1 product was assimilated in the ISBA land surface model using the LDAS-Monde tool. The experiment was conducted over Europe over the 2008-2018 time period. It was shown that the assimilation efficiently reduces the difference between SWE simulations and observations. Assimilating the CCI SWE helped reducing the model cold bias of ground temperature at all depths (1 m, 2 m, 5 m, 10 m) at high latitudes with respect to the CCI PERMAFOST mean annual ground temperature (MAGT) product.

A more detailed report of the work carried out in this sub-work package will be provided in the final version 3 of this document.

Publications

None so far, but the interest in the results leading to a journal or conference publication will be described in the next version of this report.

Interactions with the ECVs used in this experiment

The snow-permafrost cross-cutting evaluation was presented at the May 2021 CSWG session and at the May 2021 Snow-CCI user workshop.

Consistency between data products

No inconsistencies between ECV products were found. Figure 3.3.1 shows that assimilating the CCI SWE helped reducing the model cold bias of ground temperature at all depths (1 m, 2 m, 5 m, 10 m) at high latitudes with respect to the CCI PERMAFOST mean annual ground temperature (MAGT) product.

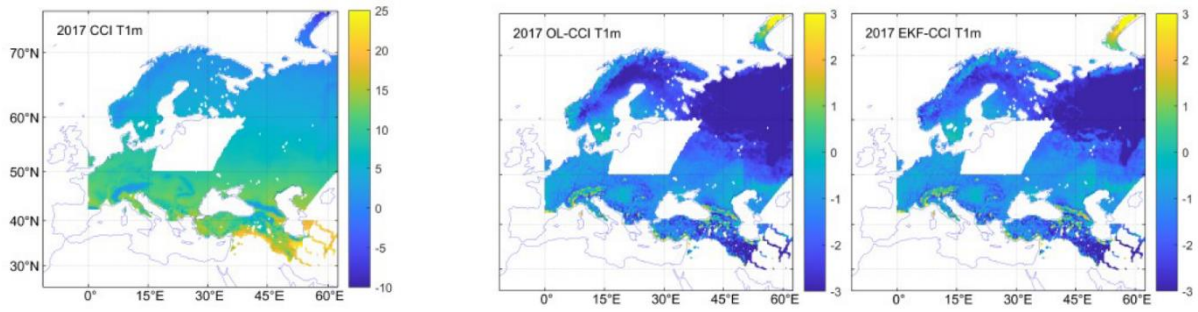

Figure 3.3.1*: Mean annual ground temperature at a depth of 1 m over Europe: (left) CCI PERMAFROST, and difference between (middle) model open-loop and CCI PERMAFROST, (right) model analysis and CCI PERMAFROST.*

Figure 3.3.2 shows that changes in the SWE annual cycle caused by the integration of SWE observations into the ISBA model have a marked impact on ground temperature at a depth of 1 m. The impact is less at 5 m but is still noticeable. The larger SWE values triggered by the assimilation tend to warm the soil.

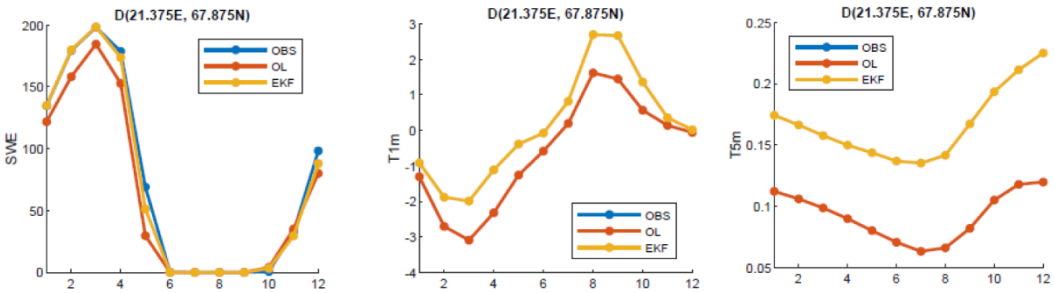

Figure 3.3.2*: Impact of (left) the assimilation of SWE on the simulated ground temperature at depths of (middle) 1 m and (right) 5 m deep soil layers over a model grid cell located at the East of Kiruna.*

Recommendations to the CCI ECV teams

Using the ISBA land surface model, it was shown that a long spinup of at least 200 years is needed to achieve ground temperature equilibrium in permafrost areas. The PERMAFROST dataset could be used in climate models to reduce the spinup time. The PERMAFROST ATBD (Algorithm Theoretical Basis Document) it should indicate how equilibrium is achieved and to what extent it is achieved.

Plan for Year 3

Work together with the PERMAFROST team in order to validate the ISBA simulations using ground observations.

3.4 Propagation of CCI(+) observational uncertainties to climate model scales

Lead partner: BSC
Authors: Aude Carreric, Markus Donat, Pablo Ortega and Etienne Tourigny

Aim

Observational uncertainties originate from a cascade of errors in the retrieval process, structural uncertainties in the algorithms, and statistical uncertainties in the spatio-temporal projections (Merchant et al., 2017). These errors are correlated in space and time, due to mesoscale systems, for instance, that impact satellite retrieval on a given spatio-temporal scale. Observational uncertainties cannot therefore be averaged and scaled by the square root of the number of independent samples as for uncorrelated errors, but require the consideration of the correlation of errors in space and time. A novel approach how to achieve this has been presented in Bellprat et al. (2018) and applied to the CCI sea-surface temperature (SST) dataset. This task will aim at expanding this effort to other CCI ECVs (all relevant to the study of wild fires) in order to disseminate propagated observational uncertainties at daily, monthly, decadal and climatological scales as well as for different grid resolutions, regions, hemispheric and global averages. It will address the following scientific questions:

1. How can the observational uncertainty estimates provided by CCI(+) reference datasets be translated into different spatiotemporal scales to compare to climate model simulations?
2. Are there important differences relative to the nature of the products?

Key Outcomes of CMUG Research

1. Results suggest that observational uncertainty on Arctic SICs can have a strong impact on the assessment of seasonal forecasts, larger than the uncertainty related to the limited ensemble size and the length of the forecasts.
2. An interesting region to study the effect of the propagation of errors for the fire ECV (burnt area) is North Australia.

Summary of Results

Deviation of plans:
The analysis on the propagation of errors started in the 1st July 2019, after the hiring of Aude Carreric (who has performed the analysis), and it has finally been centered on two ECVs: fires (i.e. burnt area) as initially planned, and sea ice (i.e. sea ice concentrations; SIC) in substitution of the originally envisaged soil moisture, for which only trajectory based L2 datasets are currently available through the CCI data portal, thus complicating the propagation into the model scales, which are gridded in space[1]. We believe that sea ice concentrations are an excellent alternative of greater utility for our ongoing activities, in which sea ice plays a central role, and the propagated errors will be more easily exploitable, as for example in the evaluation of the forecasts with the enhanced sea ice reanalysis performed in Work Package 3.8. The new ECV Land Surface Temperature has not been finally

[1] CMUG acknowledge that more datasets are available than are published on the CCI data portal and CMUG always contact the ECV teams to check if such datasets are available.

considered as the data were not available at the time the analysis started, and the allocated resources to complete this WP have already been used.

Arctic Sea Ice prediction case study:
The analysis of SICs has been focused on the Barents and Kara Seas in September and October (red area in Figure 3.4.1), a region and a season in which sea ice variations have been linked with other remote impacts, including on the North Atlantic Oscillation (e.g. Ruggieri et al 2016) and the occurrence of extremes over Europe (e.g. Acosta-Navarro et al 2019).

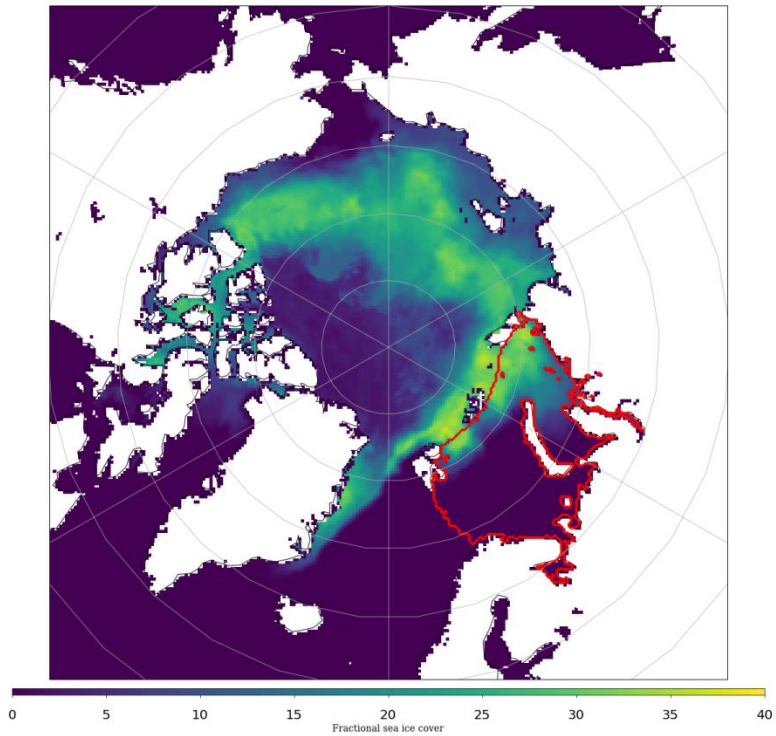

Figure 3.4.1*: Interannual standard deviation of the observed SICs (in colours) from the in August and September over the period 2003-2016. The red line encloses the Barents and Kara Seas. ESA observational data from SIC climate data record from the AMSR-E and AMSR-2 instruments at 50km grid spacing, version 2.1.*

We followed the methodology and equations in Bellprat et al. (2017) to propagate the uncertainties of SICs (from the Sea Ice Concentration climate data record from the AMSR-E and AMSR-2 instruments at 50 km grid spacing, version 2.1) into the model scales, in this case for EC-Earth 3.2 in its standard resolution (approximately 1° in the ocean). We concentrated on the average of SICs over the Barents and Kara seas and propagated the corresponding uncertainties to investigate their impact in the evaluation of skill for a seasonal prediction system with EC-Earth 3.2. This forecast was initialized every 1st May for the reforecast period 1993-2014. We also assessed the sensitivity of the skill scores, their effect compared with that of the uncertainty related to the ensemble size and the length of the forecast period (see Bellprat et al. (2017) for further details).

Figure 3.4.2 shows that the observational uncertainties have indeed a strong impact on the skill, especially for the longer lead times. In August, for example, anomaly correlation coefficients range

from 0.7 (which would correspond to very good performance) to negative values close to -0.4 (which are suggestive of really poor performance). This effect is comparable to the combined effect of the ensemble size and hindcast length uncertainty. Such results thus highlight that the skill over this area is particularly uncertain, at least for the seasonal forecasts considered. It is therefore important to identify other regions and seasons for which the skill remains high and is less sensitive to all these uncertainty sources. It is also possible that to reduce the impact of the observational uncertainty on the skill, longer reforecast periods and larger ensembles are needed, as both are expected to improve the overall skill by allowing to better constraining the predictable signals. Other potential ways to reduce the sensitivity of the skill score estimates to the observational uncertainty is to improve the initial conditions, e.g. through the assimilation of new observational products, as was done in WP3.8

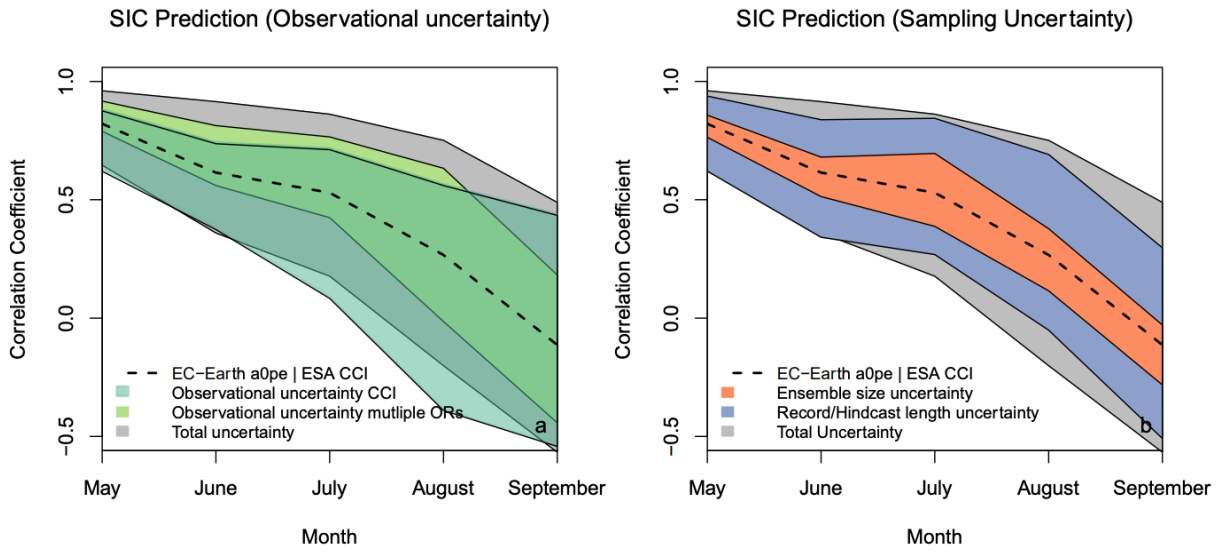

Figure 3.4.2: *Sub-seasonal to seasonal forecast skill of EC-Earth3.2 (10 members) with respect to ESA-CCI SIC (dashed line) in predicting the average sea ice concentration in the Barents and Kara Seas in a seasonal forecast system initialised on the 1st May. The areas show the 5-95% percentile range of the bootstrapped (10^6) uncertainty sources around the sample correlation skill for (left) the uncertainty in the ESA-CCI SIC observations once propagated into the model scales (blue) and the uncertainties as derived from the comparison of three other SIC products (green; NSIDC51, NSDC79 and an earlier version of ESA-CCI SIC) and (right) the sample uncertainty due to a limited ensemble size and record length of the ESA-CCI SIC product. The grey area shows the total uncertainty obtained by resampling all sources at the same time.*

Wild-fires in Australia case study:
In this study the errors were propagated into the model scales to evaluate the realism of the EC-Earth model when simulating the burned area.

The observational product considered for the burned area is ESA CCI (main product): version 5.1, from 01/2001 to 12/2018, 0.25º regular spatial resolution, monthly temporal resolution. This product was used to evaluate the simulated burned area in a historical experiment performed with EC-Earth and forced by the ERA5 reanalysis, for which we have accumulated annual values of burned area over a Gaussian grid that has a nominal resolution of 1°.

For the evaluation we used the fraction of burned area (and not the total burned area itself) because the analysis requires comparison of surfaces of different grids, and the regridding process (from the 0.25º regular resolution in observations to the Gaussian grid in the simulation) can introduce important interpolation errors in the computation of areas. It has been assumed that an area that has already burned does not have time to regenerate and burn again within the calendar year. The direct consequence of this assumption is that the total burned fraction in the year cannot be more than 100%. This assumption is not entirely correct in some grid-points, such as in Northern Africa (Central African Republic, South Sudan, Ethiopia) for instance.

A simplified diagnosis of the impact of the propagation of uncertainties on the burned area fraction has been made. All observational data were annually summed to match the simulated values. The regions of the world with the largest interannual variability in burned area (Figure 3.4.3) are Africa and Australia. In the following we focus exclusively on Northern Australia as this is a region where most wild fires are rarely human induced. This is particularly interesting as only wild fires of natural origin, or with a strong natural component can be expected to be reproduced by the model.

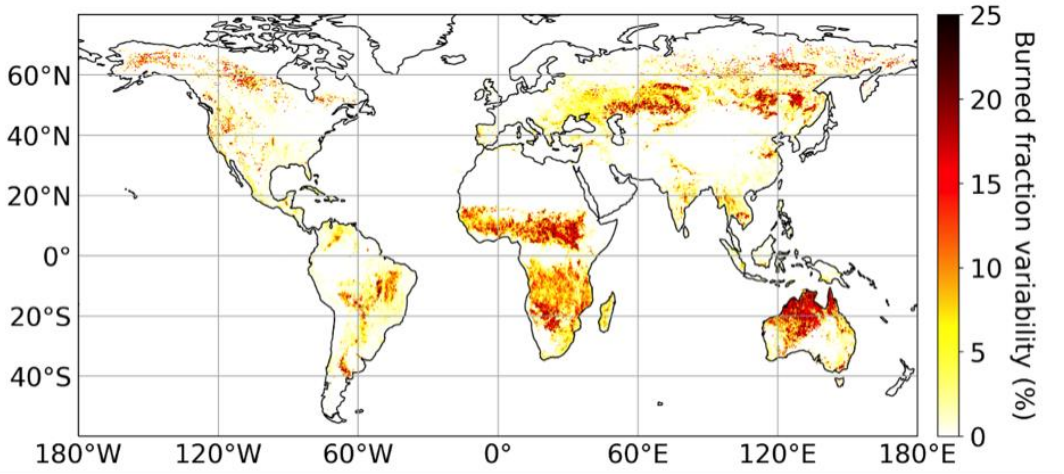

Figure 3.4.3: *Standard deviation over the 2001-2018 of the annual fraction of burned area in the CCI ESA product v5.1.*

To determine the propagation coefficient for observational the errors, their time and space decorrelation lengths are necessary. The decorrelation time of errors has been calculated from monthly errors (Figure 3.4.4), and corresponds to 1-2 months when calculated from monthly data.

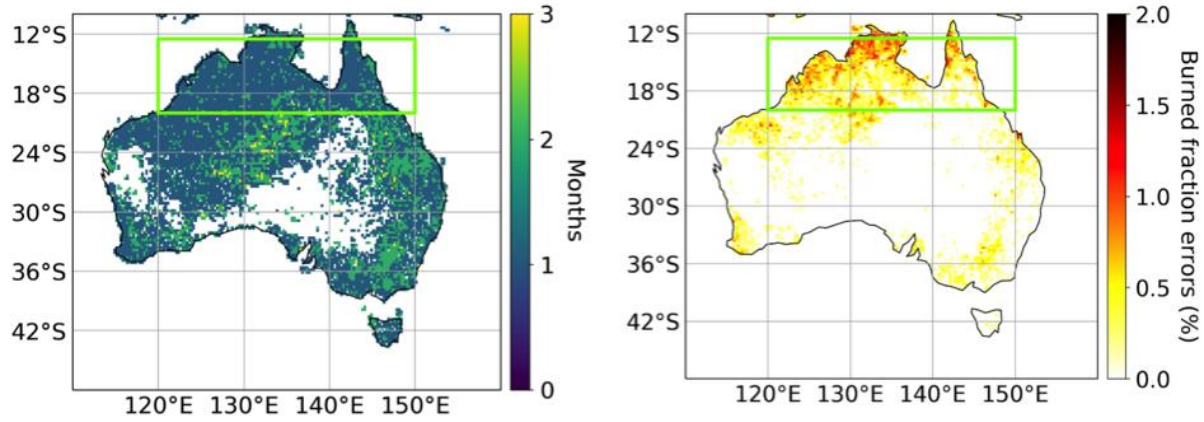

Figure 3.4.4: *(Left) Decorrelation timescales of monthly ESA CCI errors anomalies of burned area fraction, for all months (2001-2018). The decorrelation time corresponds to the first decay of an e-factor in the autocorrelation function. (Right) Observational uncertainties of the burned area fraction for the year 2015 in Australia (ESA CCI product v5.1 in its native grid).*

Since the spatial length of the decorrelation of burned area fraction errors was not provided in the documentation of the CCI dataset, we applied different choices of coherent spatio-temporal decorrelation scales to the analytical method developed in Belprat et al. (2017), that was used to compute the propagation coefficient following its Equation 3. We retained the largest (and therefore more penalising) resulting value of the propagation coefficient to perform the propagation of uncertainties to the model scales.

The propagated uncertainties (Figure 3.4.5a) were finally used to compare the climatology maps, calculated for the period 2001-2017, for the observed (Figure 3.4.5b) and simulated (Figure 3.4.5c) burned area fraction. This comparison revealed that, for all but one of the grid points, the model climatology was inconsistent with the observed one under its uncertainty range. This is a critical problem in the model that questions its use for predictive purposes.

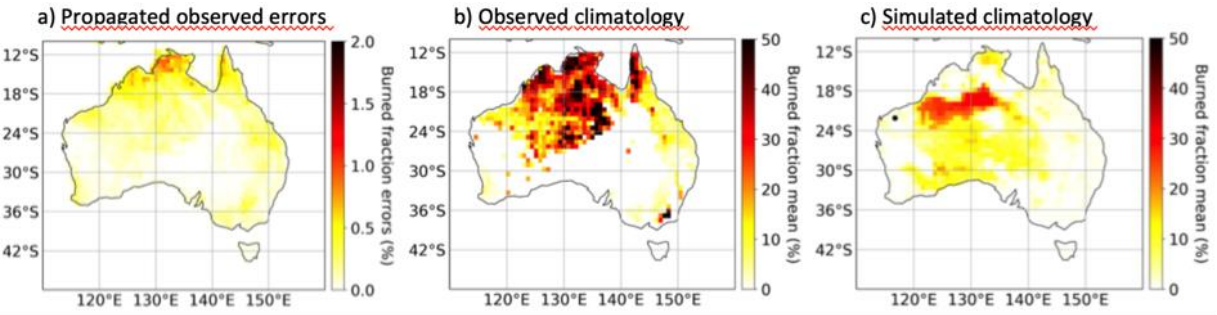

Figure 3.4.5: *a) Propagated observational errors of the fraction of burned area from the ESA CCI v5.1 product. b-c) Spatial climatology (2001-2017) of the fraction of burned area in the ESA CCI v5.1 observations and the EC-Earth historical reconstruction. The observed have been interpolated into the model grid. The black dot in panel c represents the only grid point in which the simulated mean value is consistent with the observed one when the observed uncertainty is considered.*

Publications

No new publication is envisaged of these results. The methodology applied was developed by Bellprat et al. (2017) in the previous phase of CMUG.

Interactions with the ECVs used in this experiment

During the time this work was performed there have been interactions with the SI and Fire CCI ECV teams at the quarterly CSWG meetings and the Integration meetings.

Consistency between data products

This section will provide a record of any inconsistencies found between ECV products, and will be completed in the next version of this report.

Recommendations to the CCI ECV teams

To be completed in next version of this report.

Plan for Year 3

The scientific part of this work package has been concluded. Additional feedback on aspects like consistency between the data products and recommendations to the CCI ECV teams will be provided in the final version of this deliverable.

3.5 Document SM-atmosphere feedbacks in transition regions (temperature and precipitation)

Lead partner: IPSL
Authors: Frederique Cheruy, Agnes Ducharne, Y. Zhao

Aim

The aim of this research is to examine if CCI(+) data can be used to detect the soil moisture/surface temperature feedback related to soil thermal inertia. It will address the following scientific question:

- Can the co-variations of SM, LST and precipitation be used to document the soil moisture - temperature feedback (intra-daily time scale)?

Summary of Work

Land surface temperature, soil moisture, precipitation observations have been combined on a daily basis in order to detect the contribution of soil thermal inertia which is strongly dependent on soil moisture to daily variations in night-time minimum temperature. To limit the potential sources of variation in the diurnal cycle of land surface temperature, we chose to focus on dry periods of at least 10 days at the TRMM resolution (0.25 degree) scale. In order to assess the sensitivity of the amplitude of the diurnal cycle to soil moisture during these periods we restricted the study to points where at least 16 observations per day were available. This leads us to take into account mostly cloudless days and thus limits the sources of variability of the surface temperature linked to variations in sunshine caused by the presence of clouds. The dataset used is described in Table 3.5.1: the LST pixels (0.05 degree x 0.05 degree spatial resolution) present in each TRMM grid box (0.25 degree x 0.25 degree spatial resolution) have been averaged, and data are analysed at the 0.25 degree x 0.25 degree resolution. The daily maximum LST (LST_max), daily minimum LST (LST_min) and diurnal amplitude LST (LST_amp) are calculated based on the hourly data.

The dry spell requirement combined with the requirement of having at least 16 LST values in a day, strongly reduces the number of available cases for the analysis (Figure 3.5.1). For each dry spell event, the changes between two consecutive days for LST_max, LST_min, LST_amp, SM and SWdn, (named ΔLST_max, ΔLST_min, ΔLST_amp, ΔSM and ΔSWdn, respectively) are computed. A linear regression coefficient between the change in LST (mean, max, min, amplitude) and the change in the SM is evaluated for each selected dry spell event in the TRMM grid points. The possible link between the change in max LST and change in SW radiation is also explored. Mean values of the regression coefficients are reported in Figure 3.5.2.

Table 3.5.1: Data used for the analysis.

PRODUCT	RESOLUTION	REGION	PERIOD	PLATFORM
LST CCI SEVIRI (MSG L3U)	0.05 °, Hourly	MSG disk	2008-2010	MSG2
ESA CCI SSM COMBINED (fv0 4.5)	0.25 °, daily	Global	2008-2010	Nimbus 7, DMSP, TRMM, AQUA, Coriolis, GCOM- W1, MIRAS, ERS-1, ERS-2, METOP-A, METOP-B
TRMM V7	0.25, 3 hourly	81.125 ° W-E 50° N-S	2008-2010	TRMM
CERES, V4a	1 ° , daily	Global (interpolation to LST resolution)		

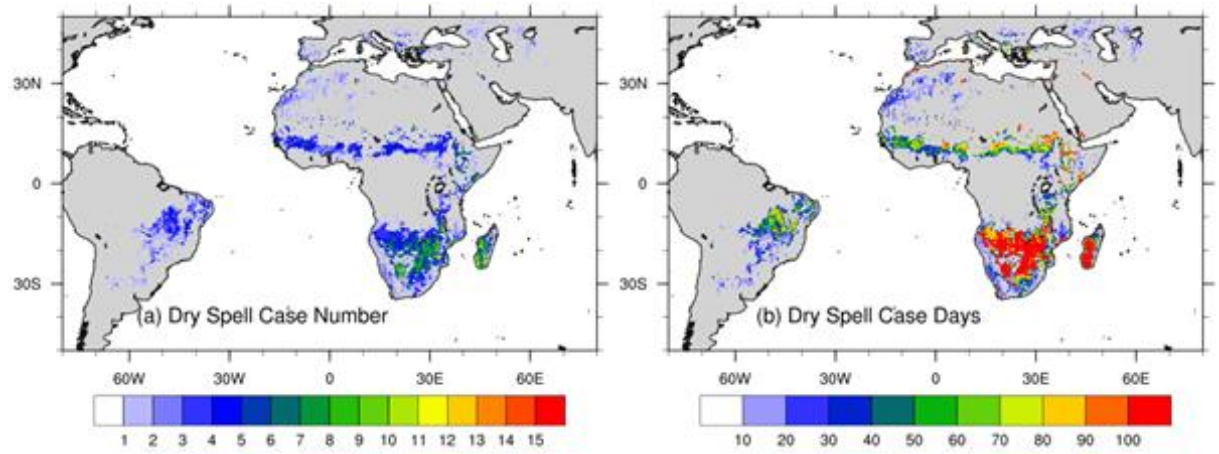

Figure 3.5.1*: Dry spell case number and number of dry spell days with at least 16 evaluations of the LST in one day (2008-2010).*

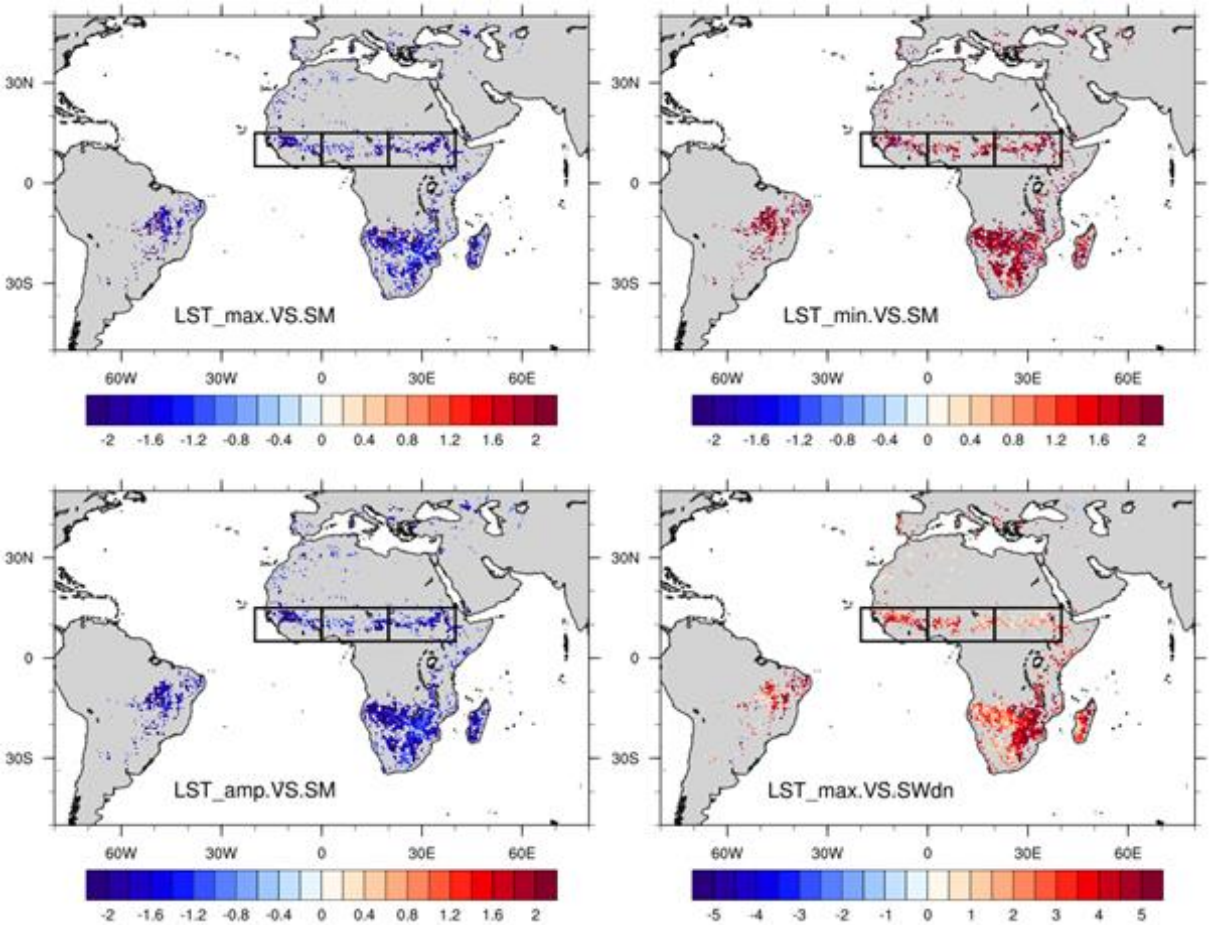

Figure 3.5.2*: linear regression coefficient between ΔLST and ΔSM (unit: 1000×(°C×m^3)/m^3), and between ΔLST_max and ΔSWdn (unit: (°C×W)/m^2). The selected boxes over Sahel are shown.*

The analysis is then conducted at the scale of the three Sahel boxes depicted in Figure 3.5.2. For each case the changes in LST_max (LST_min, LST_amp) are compared to the corresponding changes in

SM. Figure 3.5.3 shows the scatter plot of the standardized changes of these variables and confirms that an increase of SM tends to decrease the maximum LST (through evaporative cooling) and to increase the minimum LST, that is to say decrease the diurnal amplitude. This is consistent with the damping effect of the soil moisture on the nocturnal cooling through the impact of the soil moisture on the superficial thermal inertia, and to a contribution of this damping effect to the day-to-day variability of the LST. The changes in LST_max are well correlated with changes in downward SW radiation. The amplitude of the change of the LST_min, is modulated by the turbulence and the soil thermal properties (Cheruy et al. 2017), considering the normalized anomalies allows to minimize their impact.

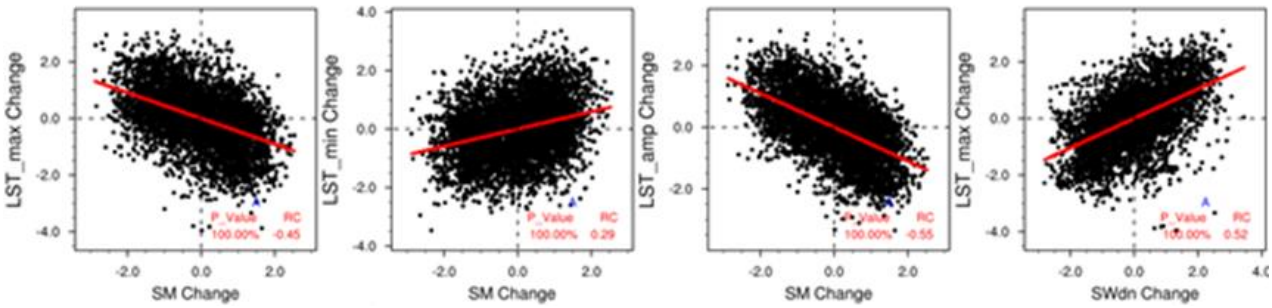

Figure 3.5.3*: Correlation between standardized ΔSM (X axis) and ΔLST change (Y axis), and between standardized ΔSWdn (X axis) and ΔLSTmax change (Y axis) over box 1 (5-15N, -20W-0E). Standardized anomalies are calculated for each selected dry spell case.*

Publications

None so far, but the interest in the results leading to a journal or conference publication will be described in the next version of this report.

Interactions with the ECVs used in this experiment

Discussions concerning the CCI-SM product took place at the Barcelona meeting (6-7 Nov. 2019, were a Poster presenting Task 3.5 results was presented). During the winter of 2019 IPSL exchanged emails with Daren Ghent to identify the most suitable LST dataset for Task 3.5. IPSL also contributed to the Climate Science Working Group (CSWG) teleconference (2020/02/04) and presented results at the CCI-LST user workshop on 24-26 June 2020.

Consistency between data products

This section will provide a record of any inconsistencies found between ECV products, and will be completed in the next version of this report.

Recommendations to the CCI ECV teams

To be completed in next version of this report.

3.6 Constraining the evapotranspiration at the scale of climate model grid-cell

Lead partner: IPSL
Authors: Frederique Cheruy, Agnes Ducharne, Y. Zhao

Aim

The aim of this research is to explore the potential of multiple satellite derived products to better understand the land surface processes and land-atmosphere coupling, at the scale of climate model grid-cells. It will mostly focus on the water and energy budgets over land, and try to identify relationships between presumably related variables, including new ECVs such as snow cover and LST. It will address the following scientific questions:

1. Can we better constrain the controls of evapotranspiration (ET) at the scale of climate model grid-cells?
2. Do the corresponding stress functions (for soil moisture, incoming energy, atmospheric humidity, temperature) take a different form at the point and grid-cell scale?
3. Can large-scale differences between LST and air temperature provide additional information to document the behaviour of parameterizations important for the near surface climate such as turbulence, heat conduction into the soil (Ait-Mesbah et al., 2015, Wang et al., 2016)?

Summary of Work

We have shown that the evapotranspiration is better constrained with a multi-layer hydrology scheme than with a *Choisnel* type scheme, however the atmospheric forcing (in coupled mode) is decisive in terms of realisms for the regional distribution of the evapotranspiration (figure 3.6.1). Concerning the snow, analysis has been done with Interactive Multisensor Snow and Ice Mapping System (IMS) data from NOAA since the CCI data were not yet available. A strong overestimation of the modelled snow cover inducing a marked cold bias in winter has been diagnosed on complex terrain such as the Tibetan plateau. This bias involves albedo-snow feedbacks and probably defects in modelling the snow cover on complex terrain (Cheruy et al. 2020).

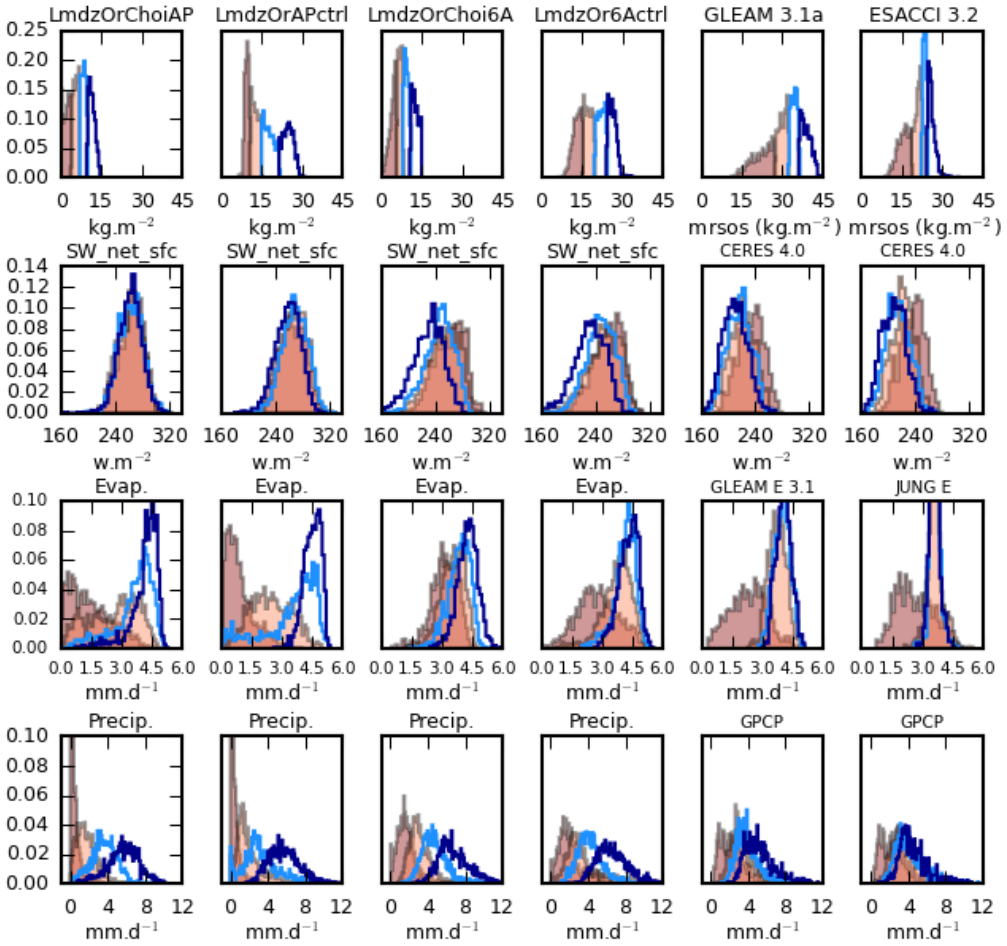

Figure 3.6.1: *Regional distribution of variables in play in the soil-atmosphere coupling, as a function of the soil moisture, modelled and observations.*

Figure 3.6.1 shows regional histograms computed on the monthly value of the individual grid points corresponding to the Southern Great Plains region (delimited with the Koeppen-Geiger climate classification) in JJA. Each row is dedicated to a particular variable relying on the coupling: superficial soil moisture (first row), net SW radiation at the surface (second row), evaporation (third row), and precipitation (fourth row). The first four columns correspond to the 4 reference experiments with different version of the GCM and land-surface model of IPSL. The first column corresponds to the configuration used for CMIP5 the last one to the configuration used for CMIP6, and the last two columns to the different sets of observations (indicated above the corresponding histograms). The colors depict the PDF from the minimum to first quartile (dark pink shade) from first quartile to the median (pale pink shade), from median to third quartile (cyan line) and from the third quartile to the maximum (blue line). (Cheruy et al., 2020, Submitted to JAMES).

Publications

Cheruy F., A. Ducharne, F. Hourdin, I. Musat,, E. Vignon, G. Gastineau, V. Bastrikov. N. Vuichard, B. Diallo, J.L. Dufresne, J. Ghattas, J.Y. Grandpeix, A. Idelkadi, L. Mellul, F. Maigna, M. nenegoz, C. Ottlé, P. Peylin, F. Wang, Y. Zhao, Improved near surface continental climate in IPSL-CM6A-LR

by combined evolutions of atmospheric and land surface physics. Journal of Advances in Modeling Earth System, 12, e2019MS002005, https://doi.org/10.1029/2019MS002005, 2020.

Interactions with the ECVs used in this experiment

In the first 12 months of this phase of CMUG work there have been interactions with the Snow, SM and LST CCI ECV teams at the quarterly CSWG meetings and the Integration meetings. This was to be informed data suitability for the work and data availability (direct from the CCI ECV teams or from the CCI Open Data Portal).

Consistency between data products

This section will provide a record of any inconsistencies found between ECV products, and will be completed in the next version of this report.

Recommendations to the CCI ECV teams

To be completed in next version of this report.

Plan for Year 3

With CCI LST and CCI Snow data now becoming available, the work should proceed.

3.7 The effect of Lakes on local temperatures

Lead partner: Met Office
Authors: Grace Redmond and Erasmo Buonomo

Aim

The aim of this research is to identify and describe the interactions and relationships between lakes and their surrounding land areas. Typically, this would be around large lakes (e.g. Victoria, Great Lakes). It will address the following scientific questions:

1. What are the interactions between lakes and the surrounding land areas?
2. What effect does lake temperature (or other parameter) have on the surrounding LST?

Summary of Work

CCI ECV lake surface water temperature and lake ice cover data are not currently useable in climate model simulations due to gaps. We suggest a reconstruction like that applied to the ARC3 lake data set (MacCallum and Merchant 2012). By including lake surface water temperature/lake ice in our re-analysis driven RCM run over Europe, winter and summer surface air temperature biases over land surrounding larger lakes (> 5000 km^2) are reduced compared to E-OBS observations. There are little to no changes in mean temperature or precipitation in areas surrounding smaller lakes (< 500 km^2) but this may be a feature of model resolution.

3.7.1 Introduction

Lakes are widely recognised to influence local climate. Lakes generally warm and cool more slowly than the surrounding land due to their higher heat capacity, this can lead to cooler summers and warmer winters, changes in precipitation and circulation. The impact a lake/s have on local climate is often related to lake size, with larger bodies of water having a much bigger impact than smaller ones (Rouse et al. 2008). Historically, lakes have not been well represented in global or regional climate models often due to low horizontal grid resolution and/or lack of observational data for validation. Approaches such as representing lakes as mostly land (Gordon et al. 2002), interpolating local sea surface temperatures and applying lake surface temperature climatologies have been employed (Mallard et al. 2005). More recently, simple lake models such as FLake (http://www.flake.igb-berlin.de) have been implemented, but results are generally compared to in situ data (Betts et al. 2020) which is not available for many lakes.

The Lakes CCI ECVs are filling an important data gap in climate observations and have the potential to improve the representation of lakes in climate models, particularly in locations where in situ observations are sparse. Our intention in this project was to use the daily lake surface water temperature (LSWT) and lake ice cover (LIC) ECVs as input to the HadREM3-GA7-05 regional climate model (RCM) over Europe at 12km horizontal resolution driven by ERA-Interim (Dee et al. 2011), the global atmospheric reanalysis product from the European Centre for Medium-Range Weather Forecasts (ECMWF) and prescribed daily sea surface temperature and sea ice from Reynolds et al (2020). For the RCM domain and land sea/lake mask, see Figure 3.7.1. However, as is described in the Results, this was not possible due to the amount of missing data (likely due to cloud) currently present in the

Lake ECVs. Instead, we used the daily ARC3 lake data set (MacCallum and Merchant 2012), which was developed as part of a previous ESA funded project. We then compared the output from the RCM experiment with ARC3 lake data, to an almost identical one where the lakes had been filled in. By comparing these two experiments we hope to 1) describe the interactions between the lakes and the surrounding land areas, and 2) to compare the different RCM experiments to observations to see how model performance is affected.

Figure 3.7.1*: RCM Land Sea/Lake Mask.*

3.7.2 Methods

Observed lake data sets

The global LSWT and Lake Ice Cover LIC ECVs are thoroughly described in the documents here https://catalogue.ceda.ac.uk/uuid/3c324bb4ee394d0d876fe2e1db217378?jump=related-docs-anchor. In summary the LSWT data was created by the University of Reading using European Space Agency (ESA), European Organisation for the Exploitation of Meteorological Satellites (EUMETSAT), ECMWF daily satellite products and has an original resolution of 0.05 degrees. The LIC data was created by H20 Geomatics from ESA and National Aeronautics and Space Administration daily satellite products with a resolution of 250m.

As is described in the Results, we were not able to use the Lake ECVs as input to our regional climate model (data gaps due to cloud). Instead, we used the ARC3 lake surface temperature data set which is derived from ESA's (Advanced) Along Track Scanning Radiometers, (A)ATSRs and Sea and Land Surface Temperature Radiometers (SLSTRs) observations. This satellite data has been through a significant reconstruction process to address the cloud cover gaps. In the ARC3 data set, Empirical orthogonal function (EOF) techniques were applied to the LSWT retrievals to reconstruct a spatially and temporally complete time series of LSWT, this process is described in MacCallum and Merchant 2012. ARC3 contains 1628 lakes and is available as a spatially complete climatology or a daily time series of per lake point data (containing one night time and one day time temperature value) from 06/1995-03/2012. The climatology would be ideal as it captures the spatial variability in temperature,

but given the significant natural variability in the region, it is not appropriate for use. Figure 3.7.2 shows the ARC3 LSWT of the largest lake in Sweden (Lake Vänern, ~5600km^2) for each year in the period 1996-2011, the day on which the lake freezes/thaws (which we assume to be when the LSWT is < 273.15K) varies by ~7 weeks. As we are using a re-analysis based on observations as boundary data to our RCM, this could lead to inconsistencies between the lake state and the surrounding air. For this reason, we use the daily per lake point data. If we were running the model over significantly larger lakes (Lake Victoria, the Great Lakes) then using point data may not be appropriate.

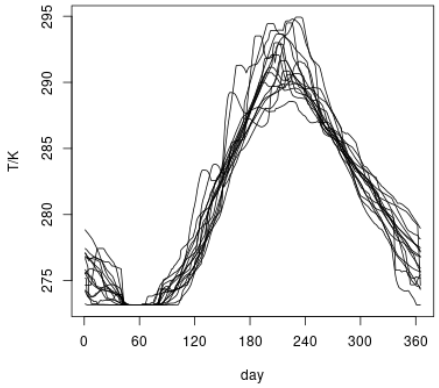

***Figure 3.7.2**: Lake Vänern daily LSWT (1996-2011) from ARC3.*

Other observations

In order to understand the impact using observed lake data has on our experiments, we compare model output for precipitation and surface air temperature to the E-OBS v20.0e data set (Cornes, et al. 2018). E-OBS is a gridded data set at 0.1 degree resolution (v20.0e) based on station observations. It has been robustly evaluated and its limitations are well described e.g. inhomogenity of stations and the underestimation of precipitation (Sevruk, 1986), it is the standard reference for RCM evaluation over Europe (Kotlarski, et al. 2019).

We also compare model land surface temperature (LST) to the Special Sensor Microwave/Imager and Special Sensor Microwave Imager/Sounder L3C v1.51 (SSM/I SSMI/S L3C) Satellite data set. The LST observations are of particular interest as they are a part of the CCI LST ECV product, the development of which is still in progress. The product specification document can be found here https://climate.esa.int/sites/default/files/LST-CCI-D1.2-PSD%20-%20i1r11%20-%20Product%20Specification%20Document.pdf. SSMI SSMIS L3C has a spatial resolution of 0.25 and is available on annually, monthly and daily timescales. There are two passes per day at roughly 6am and 6 pm, we take the average of the two passes as our LST value at each grid point. Larger bodies of water are represented by missing data, smaller lakes are often contaminated by surrounding land but still have a significantly different temperature to land only grid boxes. One of the main benefits of this product over others is that it is an all-sky data set, so there are almost no gaps. It may be less accurate than some other products that are part of the CCI LST ECV, but for our purpose this is more than made up for by the lack of gaps due to cloud.

Regional Model and experiment set up

The atmosphere only RCM HadREM3-GA7-05 was used to downscale ERA-interim re-analysis (Dee, et al. 2002) to 12km over Europe (see domain in Figure 3.7.1). The HadREM3-GA7-05 is the regional version of the global GC3.05 configuration of the Met Office Hadley Centre Unified Model and consists of atmosphere: GA7.0 (Walters et al. 2017) and land: GL7.0 (Walters et al. 2017) components. Sea surface temperatures and sea-ice extents are prescribed from analyses of observations (Reynolds et al., 2002). Model set up is described fully in Tucker, et al. 2021 (submitted) which also uses the same domain but uses interpolated SSTs for LSWT in Scandinavia and Northwest Russia. As far as possible we represented the location and shape of lakes realistically, but due to model resolution this was not always possible. For example, in south Finland several lakes were joined together and the LSWT was taken from the lake with the closest lat/lon point to the centre of the combined lake.

Two experiments were carried out, they were identical to each other except one replaced lakes with land points (referred to as the Filled Lakes experiment), and the other prescribed LSWT using daily night time ARC3 data (referred to as the ARC3 Lakes experiment). LIC data was not available so the assumption that when LSWT < 273.15, LIC = 1 and when LSWT > 273.15, LIC = 0 was made. The only other way the two runs differ is length, the Filled Lakes experiment ran from 12/1981-12/2012 and ARC3 Lakes ran from 06/1995-03/2012. The Filled Lakes experiment is part of the EURO-CORDEX initiative (Jacob, et al. 2014) and had to be run for a defined period. We discarded the first year of data (06/1995-06/1996) from the ARC3 Lakes run as model spin up and only compare data from 06/1996-03/2012 for both experiments.

3.7.3 Results

CCI Lake data

The RCM relies upon ancillaries, such as LSWT, containing no missing data at all. If there are one or two day stretches missing occasionally, or one or two grid boxes containing missing data, it is fairly straightforward to interpolate in space or time. However, in the case of the LSWT and LIC CCI data from this project, it quickly became clear that the gaps in data were far more extensive. Figure 3.7.3 is a histogram of the fraction of lake grid boxes (in the European RCM domain) that contain non-missing data each day in the period 1996-2011. All available LSWT data that isn't missing is counted as valid, including those flagged as bad data, worst quality and low quality, as well as that flagged acceptable and best quality. Particularly in winter when there is likely to be more days of cloud cover, there is a high proportion of days where there is little to no data. In DJF (JJA), ~63% (~28%) of days contain 0%-5% of non-missing data for LSWT. LIC tends to have fewer, but still significant gaps, in DJF (JJA), ~31% (~25%) of days contain 0%-5% non-missing data.

Whilst the picture is better in the summer, for LSWT only ~0.6% of days contain >80% non-missing data. The gaps due to cloud are often spatially variable, you might have all grid boxes containing data for one lake, but another in the domain has no data; there are also occasions where the majority of lakes contain a couple of grid boxes of data but are otherwise missing. We also looked briefly at the global picture in case our domain choice was particularly unfortunate to contain a lot of gaps, but it did not change our conclusion that at present, the LSWT and LIC are not able to be used as input to

prescribe lake surface properties in climate models, and would be of very limited use to validate RCM output or lake model output.

Given the current unsuitability of the CCI Lakes data to prescribe LSWT and LIC, we looked for alternative sources of lake data with which to run our RCM experiments. We used ARC3, developed as part of a previous ESA project. ARC3 also contained gaps due to cloud cover, but a complex reconstruction detailed in MacCallum and Merchant 2012. ARC3 demonstrates what would be possible if the gaps in the Lake CCI data were addressed. Following a positive outcome of this study, we would strongly recommend that a similar reconstruction be tested and applied by observation scientists in the next phase of the project in order to make the Lake CCI data more useful to the climate modelling community.

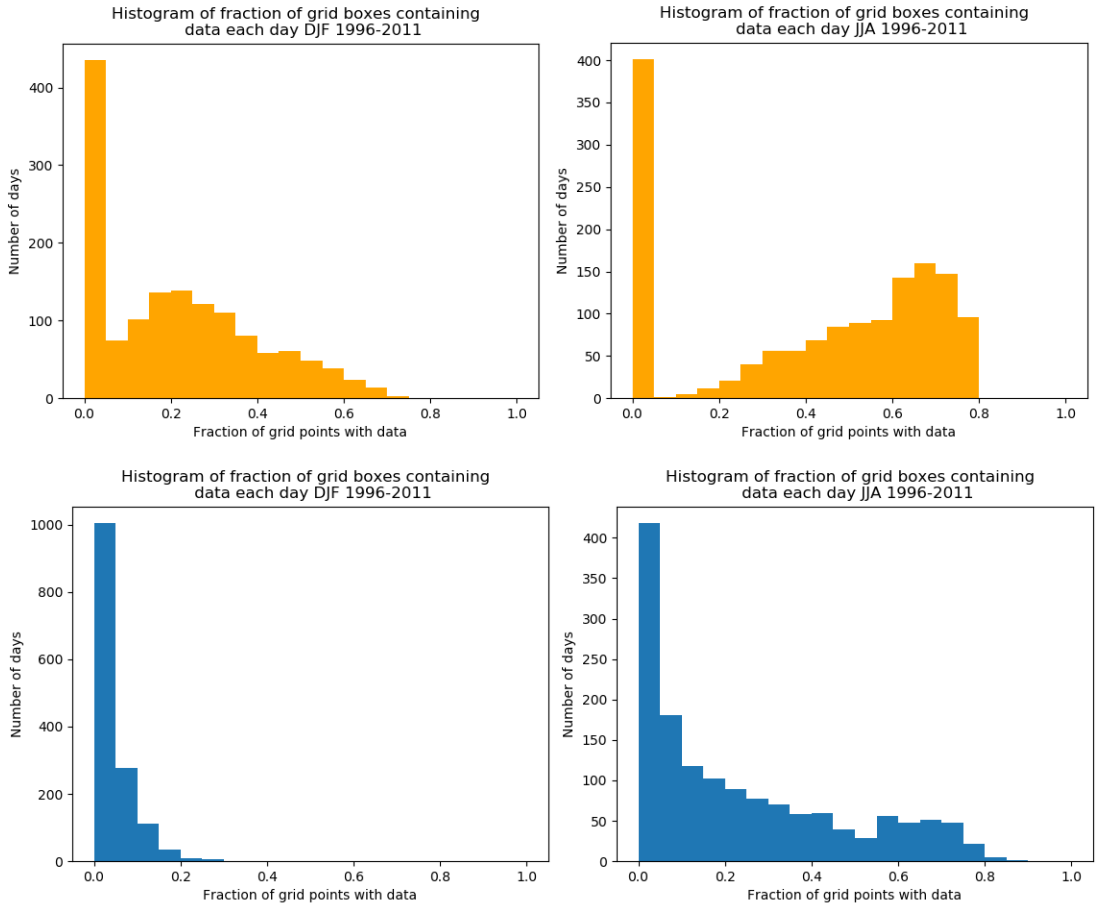

Figure 3.7.3*: histograms of the fraction of grid boxes containing data (i.e. not missing) each day in the European RCM domain for the period 1996-2011 LIC (orange) and LSWT (blue)*

RCM results

Figures 3.7.4 and 3.7.5 show the seasonal mean surface air temperature for DJF over the period 12/1996-2/2012 for E-OBS observations, the two RCM experiments (ARC3 lakes and Filled lakes), and the differences between them over the whole domain and a section which spans 54°-65°N and 10°-39°E. There is a ~3°C cold bias over Norway, the Alps, Russia and North Africa with respect to E-OBS in both the ARC3 lakes and Filled lakes RCM experiments (Figure 3.7.4). We are mostly

concerned with the impact of adding lakes, but these biases are comfortably within the range of biases found ERA-interim driven RCMs over the same domain (see Kotlarski, et al, 2014 for a detailed comparison).

The bottom right plot in Figure 3.7.4 shows the difference between ARC3 lakes and Filled lakes simulations. There are large temperature differences over the lakes, with the ARC3 lakes simulation being 2ºC-5ºC warmer than Filled lakes simulation. This is mostly in line with what we would expect given the higher heat capacity of water compared to land. Over the smaller lakes (we somewhat arbitrarily define a smaller lake as those which as <500km^2), the temperature difference is generally confined to the lake itself, however over larger lakes (defined as those >5000km^2) in Sweden, South Finland and particularly Russia, the air temperature over the land surrounding the lakes is also higher. This can be seen in Figure 3.7.5, which is a section of the domain containing the largest lakes. We have masked out the lakes in order to more easily see the effect on the surrounding land. The air temperature immediately surrounding the Swedish lakes is ~0.5ºC warmer in the ARC3 lakes experiment. The air temperature around the Russian and Finnish lakes is 0.5ºC-2.5ºC warmer in the ARC3 lakes experiment, the impact on air temperature over land decreases the further you are from the lake, but it extends several hundred kilometres in each direction. The cold bias over Russia and south Finland with respect to E-OBS is reduced by up to 3º and in south Finland has become a warm bias.

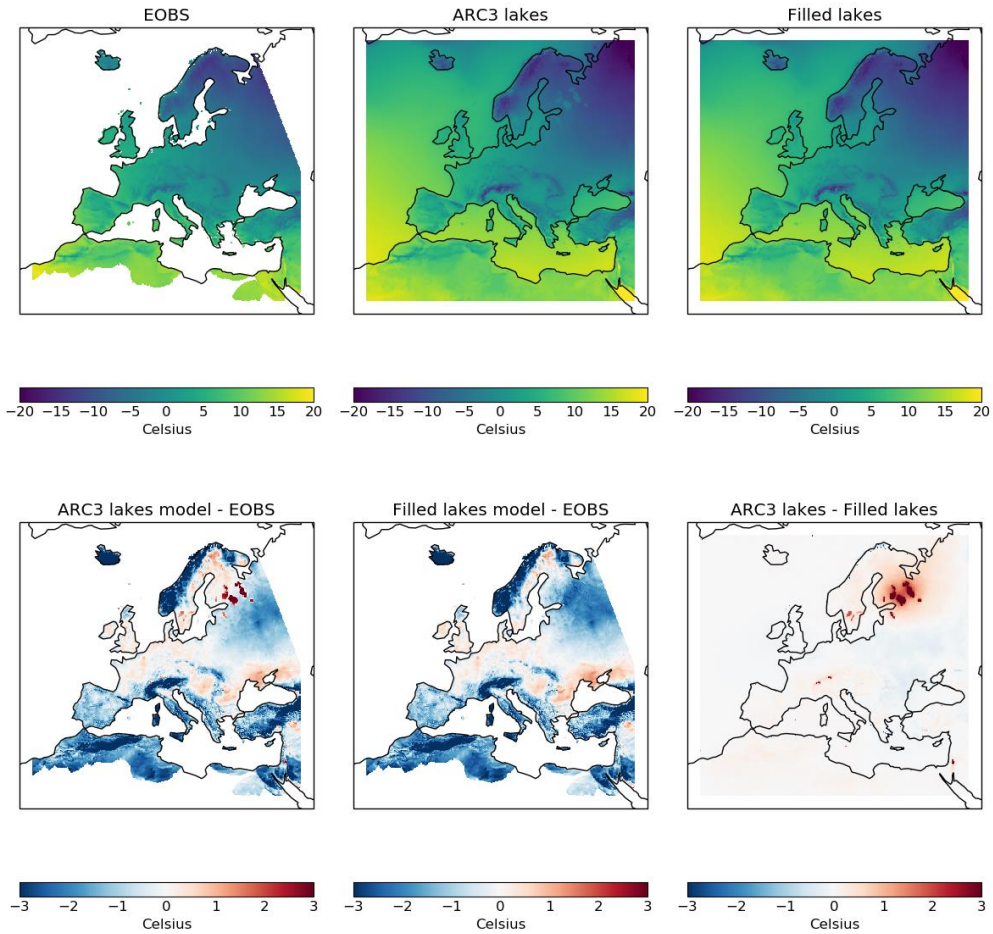

Figure 3.7.4: *DJF seasonal mean (1996-2012) surface air temperature for: E-OBS, ARC3 lakes simulation, Filled lakes simulation and the respective differences between them.*

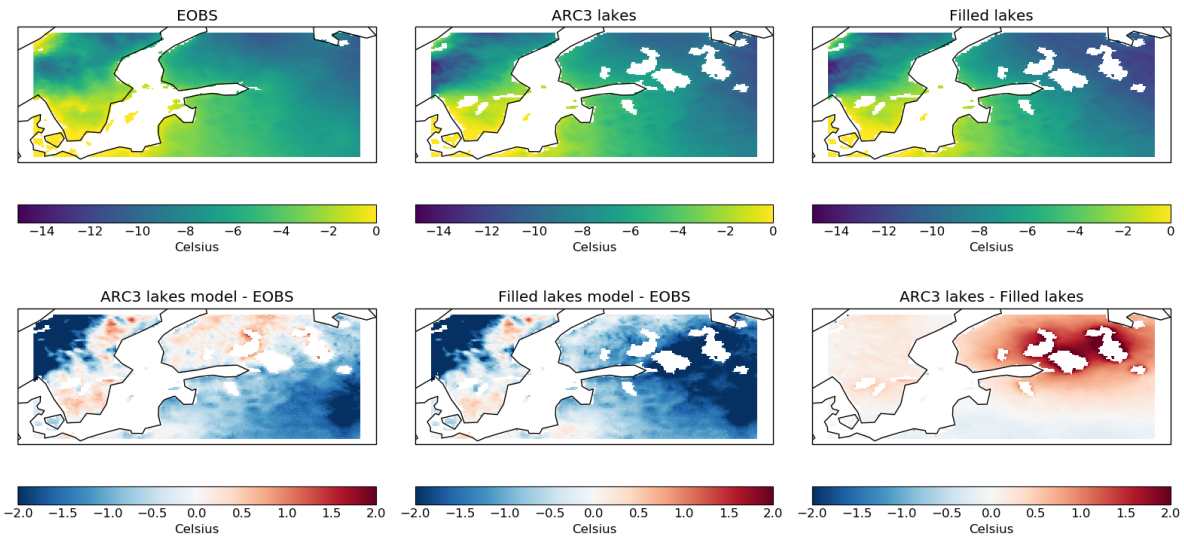

Figure 3.7.5*: DJF seasonal mean (1996-2012) surface air temperature with RCM lakes masked out for: E-OBS, ARC3 lakes simulation, Filled lakes simulation and the respective differences between them.*

Figure 3.7.6 shows the seasonal mean surface air temperature for JJA over the period 12/1996-2/2012. There is a warm bias of up to 3^{o}C over Southern and Central Europe and North Africa which is again within the range of biases seen when downscaling ERA-interim using an RCM (Kotlarski, et al, 2014). The air temperature difference between the ARC3 lakes and Filled lakes simulations in summer is much less pronounced than in winter, the small lakes in Italy have temperatures similar to that of the Filled lakes run. The Swedish, South Finnish and Russian lakes are cooler in the ARC3 lakes experiment by 1^{o}C-3^{o}C. The ARC3 lakes simulation is generally ~0.5^{o}C warmer over Central Europe than Filled lakes, this bias is currently unexplained, it could be related to the addition of lakes in a non-obvious way, or it could be due to the differing run lengths between the models.

The air temperature over land surrounding the Russian and South Finnish lakes is up to 1^{o}C cooler in the ARC3 lakes simulation than the Filled lakes simulation (Figure 3.7.7). This reduces the RCM's warm bias compared to E-OBS and in some areas becomes a slightly cool bias. The air temperature surrounding the Swedish lakes is very similar in both experiments, with the ARC3 simulation lakes being slightly warmer (~0.3^{o}C). The temperature difference between the Swedish lake region from the ARC3 lakes and Filled lakes simulations is much smaller than that of the Russian lakes from the same simulations (1^{o}C vs 3^{o}C). The greater the temperature difference between the Filled lakes and ARC3 lakes, the greater the impact on the air temperature over land.

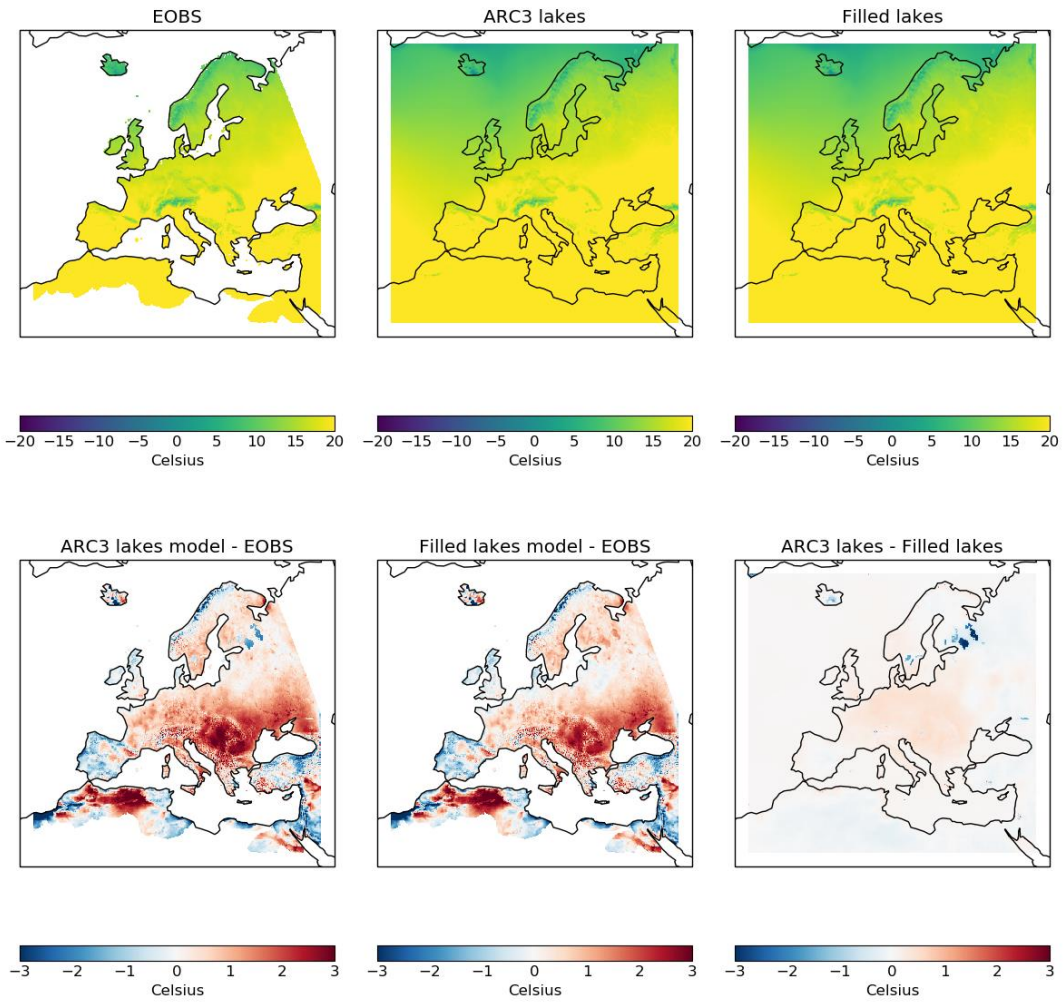

***Figure 3.7.6**: JJA seasonal mean (1996-2012) surface air temperature for: E-OBS, ARC3 lakes, Filled lakes and the respective differences between them.*

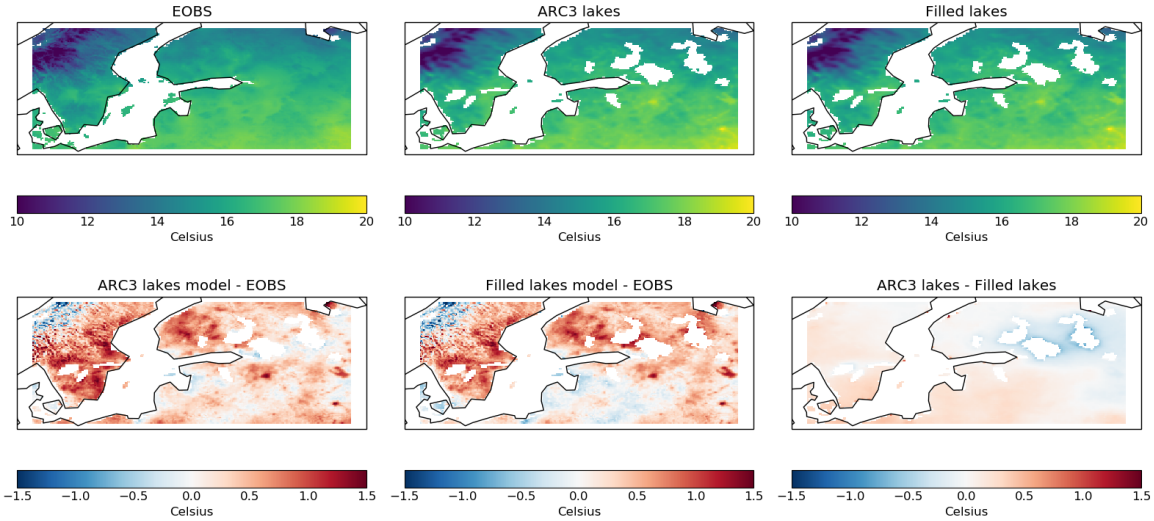

***Figure 3.7.7**: JJA seasonal mean (1996-2012) surface air temperature with RCM lakes masked out for: E-OBS, ARC3 lakes simulation, Filled lakes simulation and the respective differences between them.*

Figure 3.7.8 shows the seasonal mean of winter precipitation for the larger lakes in the domain (with the lakes masked out). In the wider domain (figures not included), there is a wet bias of ~25%, and E-OBS is known to under-catch precipitation, particularly over complex orography (Kotlarski, et al. 2019). Precipitation over land surrounding the larger lakes is slightly increased (0.5-1 mm/day) in the ARC3 lakes experiment compared to the Filled lakes experiment. This makes intuitive sense given the presence of a warmer water body increasing evaporation and moisture.

The opposite is true in JJA (Figure 3.7.9), where it is generally drier over the land surrounding the lakes (up to 1mm/day). It is possible the reduction in precipitation is due to decreased evaporation (the ARC3 lakes simulation is cooler than the Filled lakes simulation), but there was not time to properly investigate the cause. This drying slightly reduces the wet bias with respect to E-OBS. In the wider domain, there is a summer wet bias in Northern Europe and over the Alps (similar magnitude to winter), and a smaller dry bias in Central Europe. There is a small increase in cloud amount (figures not included) over the larger lakes of up to ~3% in the ARC3 lakes run, but there are similar sized differences elsewhere in the domain so it is not possible to attribute these to the addition of lakes without further work for which there was not time.

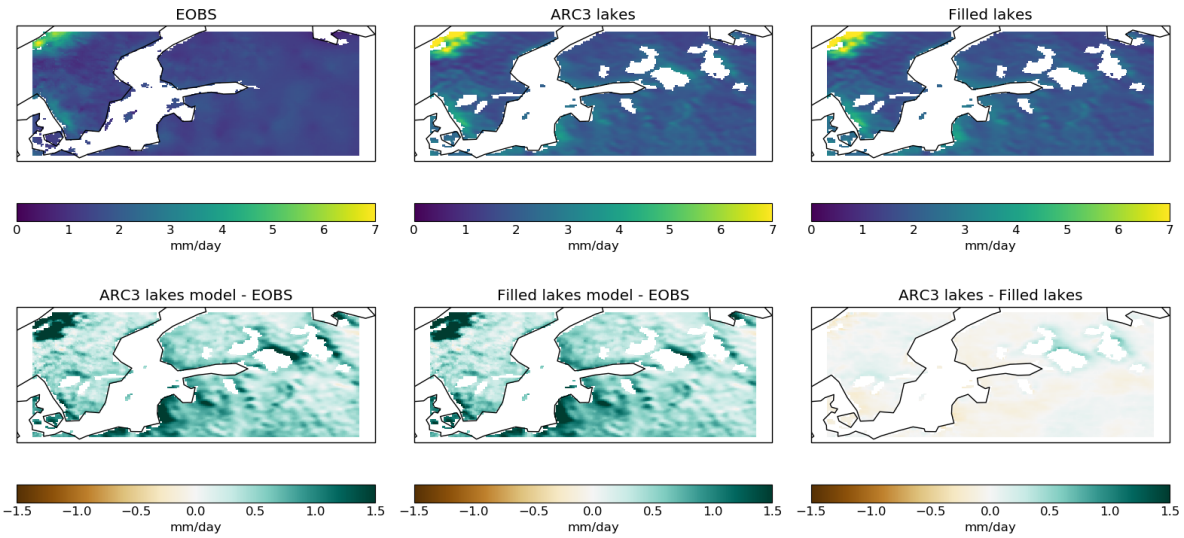

Figure 3.7.8*: DJF seasonal mean (1996-2012) precipitation with RCM lakes masked out for: E-OBS, ARC3 lakes, Filled lakes and the respective differences between them.*

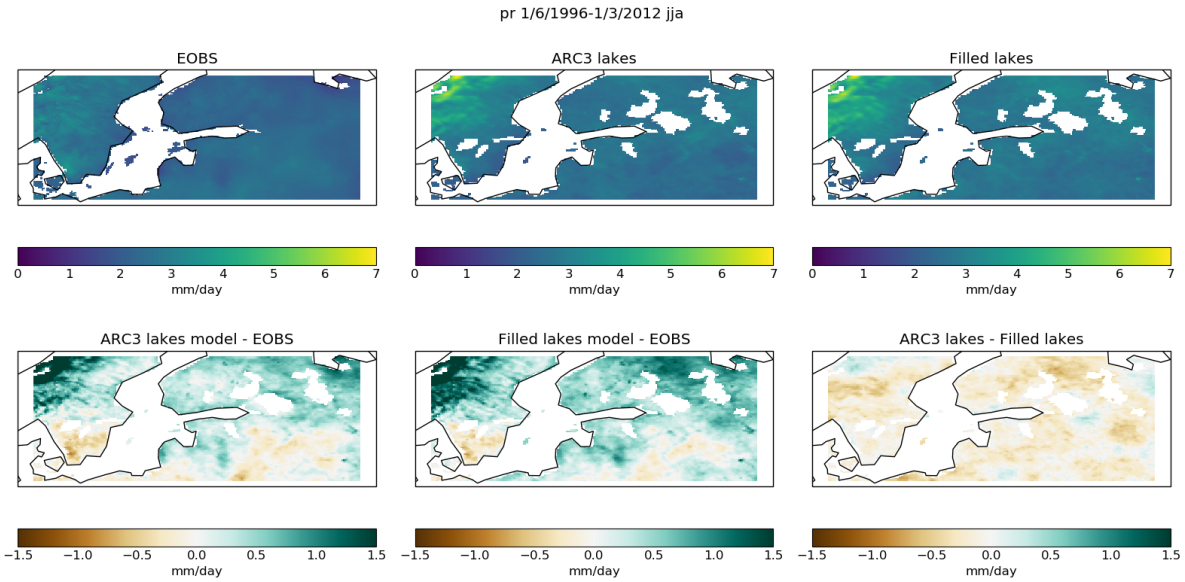

***Figure 3.7.9**: JJA seasonal mean (1996-2012) precipitation with RCM lakes masked out for: E-OBS, ARC3 lakes, Filled lakes and the respective differences between them*

A comparison of seasonal mean skin temperature (which is equivalent to SSMI SSMIS L3C land surface temperature) is shown in Figures 3.7.10 and 3.7.11. In winter there is a significant difference between the SSMI SSMIS L3C observations and the RCM experiments (Figure 3.7.10). The RCM experiments are ~4^{o}C warmer than the observations except over the Alps, the Balkans and parts of Norway and Sweden where the RCM is cooler than the observations. This is contrary to the cool bias of winter surface air temperature in the RCM compared to E-OBS (Figure 3.7.4). Over the lakes and surrounding land areas DJF skin temperature differences between the ARC3 lakes and Filled lakes simulations are very similar to air surface temperature, with small lakes being warmer but not affecting the temperature of the surrounding land, but larger lakes, particularly in Russia and South Finland having a significant influence over surrounding land surface temperatures.
The summer skin temperature differences (Figure 3.7.11) show smaller differences between observations and RCM experiments, with a warm bias over Central Europe (similar to that seen in E-OBS surface air temperature) and bodies of water, and cool biases (~2^{o}C) over Northern Europe, Spain, Portugal and Turkey. The cooler lakes can be seen in the observations and ARC3 lakes reduces the warm bias over them compared to the filled lakes run. For DJF the opposite is true, the lakes are warmer than the surrounding land and the warm bias with respect to SSMI SSMIS L3C is exacerbated.

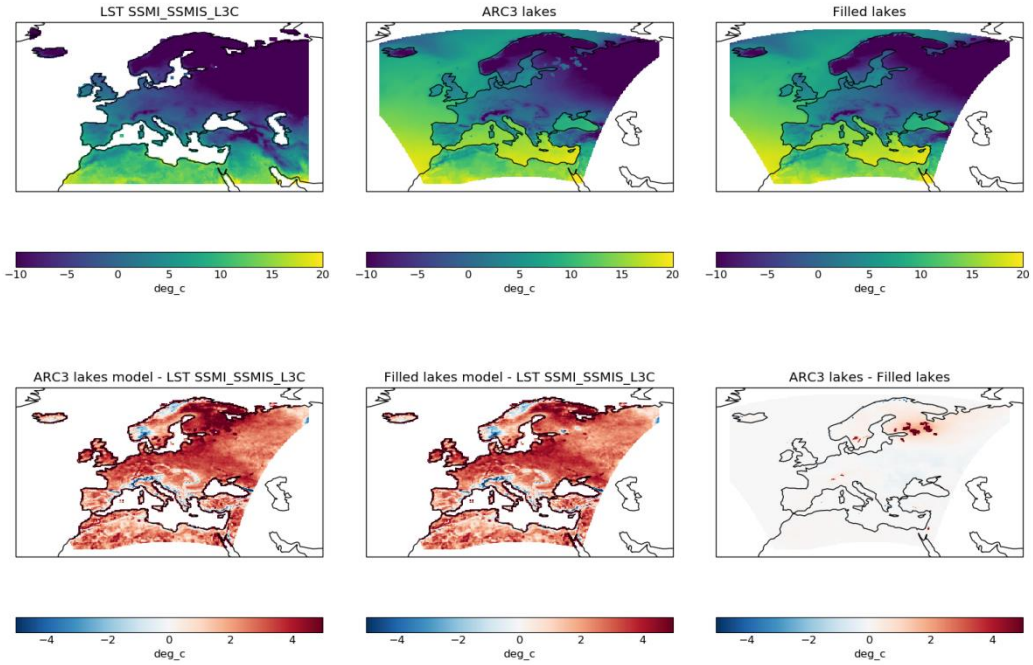

Figure 3.7.10*: DJF seasonal mean (1996-2012) skin temperature for: SSMI SSMIS L3C, ARC3 lakes simulation, Filled lakes simulation and the respective differences between them.*

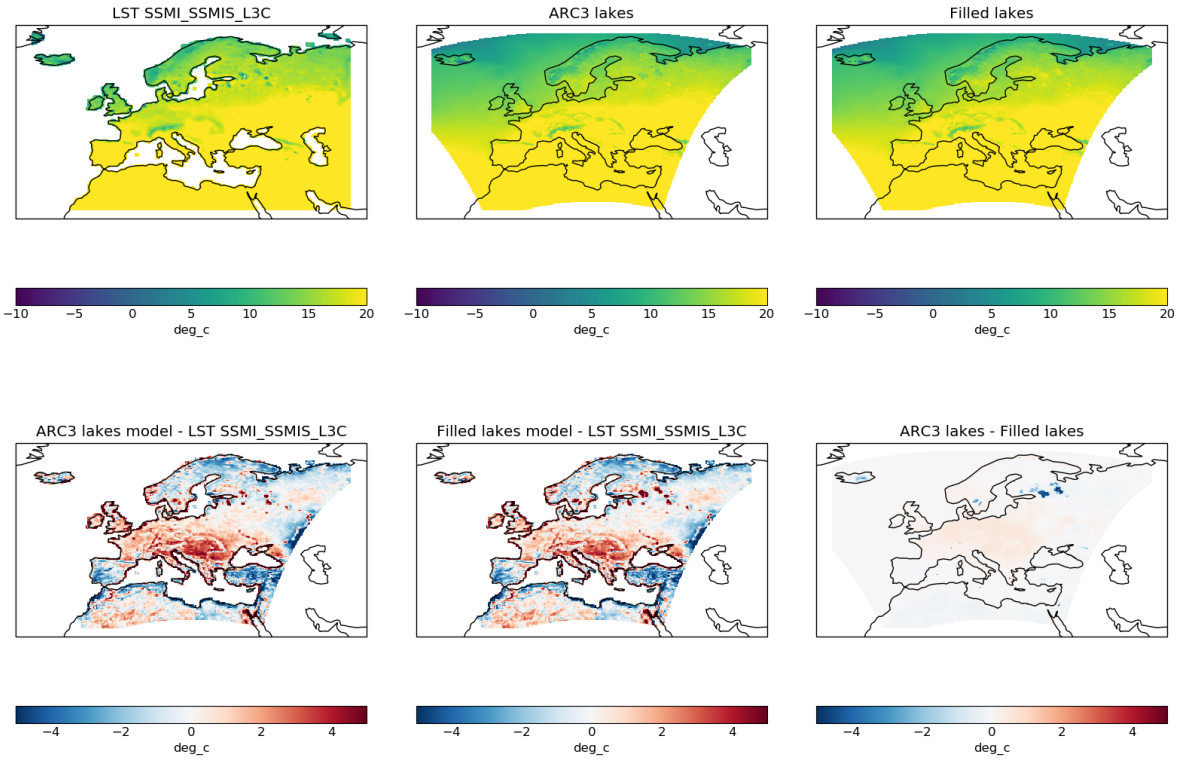

Figure 3.7.10*: JJA seasonal mean (1996-2012) skin temperature for: SSMI SSMIS L3C, ARC3 lakes simulation, Filled lakes simulation and the respective differences between them.*

3.7.4 Summary

The current CCI LSWT and LIC datasets are of limited use to the climate modelling community due to the large amount of cloud cover gaps in the data at daily timescale. This makes them unsuitable for using as model input or for robust validation of model output. However, if a reconstruction was applied as was done to a previous ESA LSWT product (ARC3), they could prove very useful indeed. It would also be beneficial if scientifically/mathematically plausible, to try to build on ARC3 by creating a spatially coherent daily time series, rather than point data. Spatial data would be particularly useful for larger lakes.

The difference between the RCM experiments demonstrates that there is a clear impact on climatological means of the surrounding air when including prescribed LSWT and LIC data. This generally only applies to larger lakes, but this could be a function of using a 12km RCM where each grid box is 144km^2. The cold bias in surface air temperature over Russia in winter (compared to E-OBS) is reduced in the prescribed lakes run, and to a lesser extent, the warm bias in summer is also reduced. There were smaller effects on precipitation. The land surrounding the larger lakes experienced more precipitation in winter, and less in the summer in the ARC3 lakes experiment compared to the Filled lakes experiment. Unfortunately, there was not the opportunity in this study to look more deeply into the interactions between the lakes and the surrounding land areas, but this would be an area of interest if there were to be any future work. Extreme precipitation and temperature indices, not included in this analysis, could also support for the improvement of the description of lakes and their coupling with the atmosphere, another aspect which could be considered in future work.

Publications

None so far, this research could be the first step in the inclusion of a lake component in the Met Office regional model, which might lead to a publication.

Interactions with the ECVs used in this experiment

Lake ECVs team helped to understand the dataset produced by this project and suggested alternative dataset which better matched the high-frequency/completeness requirement of for using lake ECVs in a regional climate model experiment. The CCI land surface temperature dataset was also used for climate model validation and the LST CCI CRG consulted on the best version of this dataset to use.

Consistency between data products

ECV lake products from CCI were not used.

Recommendations to the CCI ECV teams

The main recommendation, discussed in the main text, is to support the work needed to fill gaps in the daily LST and Lake ice datasets by a physics-based reconstruction such as the procedure used by MacCallum and Merchant (2012).

Plan for Year 3

The work using the Lakes CCI data is now complete for this phase of CMUG.

3.8 Evaluation of the impact of an enhanced ESA Sea Ice reanalysis (EnESA-SIR) on initialization of seasonal prediction

Lead partner: BSC
Authors: Juan Camilo Acosta-Navarro, Rubén Cruz-García, Vladimir Lapin, Yohan Ruprich-Roberts, Valentina Sicardi, Pablo Ortega.

Aim

The aim of this research is to quantify the benefits on forecast skill related to an enhanced initialization of sea ice (based on a reanalysis that includes both assimilation of Sea Ice Concentrations (SIC) from ESA CCI and nudging to ESA CCI ocean temperature and salinity observations). This is an improved strategy to the one previously used by the BSC, which only included assimilation of ocean temperature and salinity. The EnESA-SIR now employed should improve the prediction skill over the Arctic, and has also the potential of improving the predictions in other remote regions via some observed atmospheric teleconnections. This WP will address the following scientific questions

1. What are the benefits of initializing with the new EnESA-SIR reconstruction on the seasonal climate forecast quality?
2. Is there any added-value in the assimilation of SICs?
3. Are there any benefits for the predictive skill in remote regions? If yes, can those benefits be traced back to the assimilation of Arctic SICs?

Key Outcomes of CMUG Research

Scientific outcome: The experiments performed and analysed have revealed important benefits from the assimilation of SICs, especially in the summer season, that will be described in the following section.

Technical outcome: The model capabilities developed to enable the assimilation of sea ice concentrations through nudging have been finally implemented in the CMIP6 version of the Earth System Model EC-Earth, and will be used in all new future prediction systems developed at the BSC.

Summary of Results

Production and evaluation of the enhanced Sea Ice reanalysis:

In order to perform the reanalysis, we had first to implement some technical developments, in particular to include the nudging capabilities in the CMIP6 version of EC-Earth. The nudging module for ocean temperature and salinity was introduced in the CMIP6 version of EC-Earth at the beginning of 2019 by Valentina Sicardi and Yohan Ruprich-Robert. Later in that year, Vladimir Lapin introduced in the model an additional nudging routine to assimilate sea ice concentrations and sea ice thickness.

This module was subsequently tested, with encouraging results. Figure 3.8.1 shows that, for a nudging experiment with EC-Earth that assimilates the sea ice concentrations in July-August-September (JAS) for a future Arctic/Antarctica scenario (Smith et al. 2019), the model constrains quite accurately the target fields. Indeed, when computing the difference between the simulations and the target fields, values are always below 10% for all seasons, and are particularly small in JAS in the Arctic, with errors in the order of 2%.

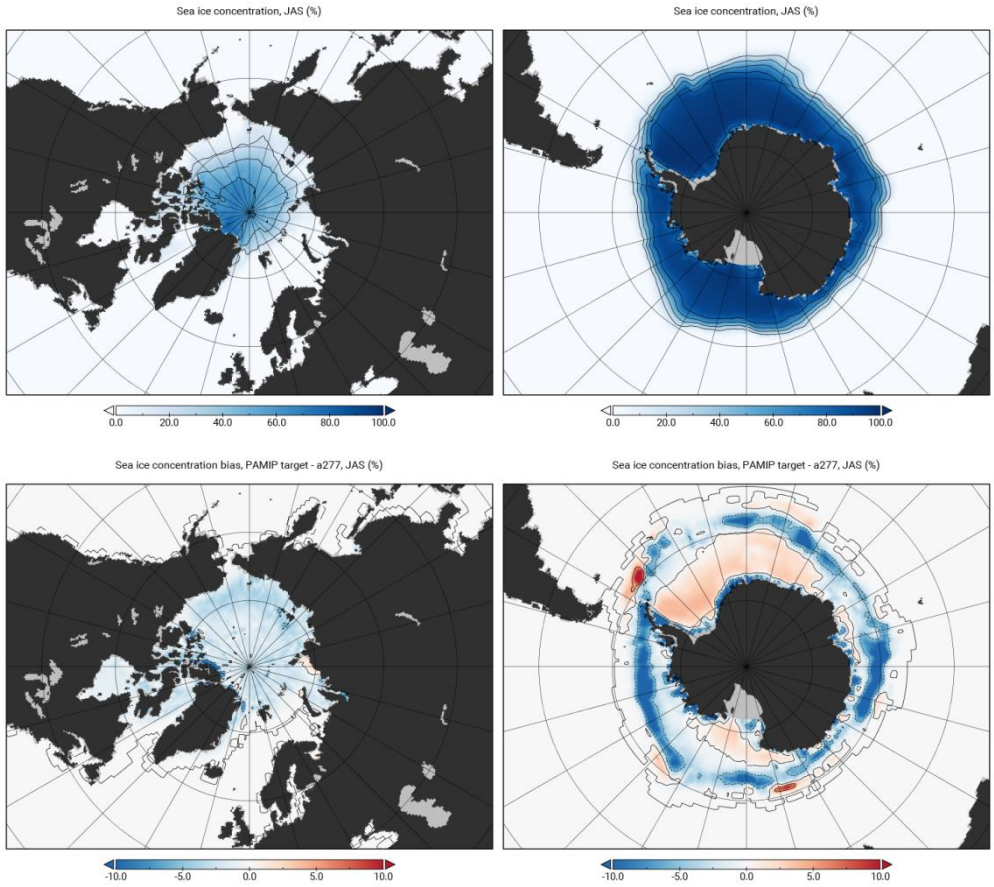

Figure 3.8.1: *(top) Average of JAS sea ice concentrations (shaded in %) in a simulation with EC-Earth3.3 that assimilates the sea ice of a future Arctic/Antarctic scenario (Smith et al. 2019; contours in increments of 20%), respectively. (bottom) Difference in JAS sea ice concentrations (in %) between the EC-Earth nudged experiment and the reference future Arctic/Antarctic sea ice concentrations, respectively.*

This same version of the model has later been used to produce two in-house reanalyses covering the period 1990-2018, one assimilating SICs, temperature and salinity (i.e., the enhanced reanalysis), and another baseline reconstruction that only assimilates temperature and salinity. In both cases the reconstructions were produced with the ocean-sea ice stand-alone version of EC-Earth, forced with surface fluxes from the ERA5 atmospheric reanalysis, and the target dataset considered for ocean temperature and salinity nudging was the ocean reanalysis ORAS5. For the enhanced sea ice reanalysis, three different members were produced, assimilating in each case a different SIC product to sample the uncertainty in the observational datasets: OSISAFv2, CERSAT and ORAS5. So far only

the SIC data assimilated in WP3.8 comes from the ESA CCI program. We plan to use SST and SSS for the skill assessment, but that will be done in the final deliverable.

Production of the seasonal predictions:
Two different sets of seasonal predictions were performed in the second half of 2020 with the coupled version of EC-Earth, the first initialised from the enhanced reanalysis, and the second from the baseline reconstruction. By construction, the comparison of both prediction systems allows to determine the impact of SIC assimilation on the seasonal predictive skill. Each system considers the re-forecast period 1992-2018 (27 years) and has 30 members, a 7-month forecast horizon and two different start months (November and May).

A first exploratory analysis revealed that SIC assimilation had a positive impact on the skill of Arctic sea ice, but mostly in the May-initialised predictions, with very marginal improvements and in some cases deteriorations of skill obtained for the November-initialised re-forecasts. This pointed to a potential issue in the nudging protocol for SIC during the winter season that is currently under investigation, and prompted us to focus the main analyses on the May initialized predictions.

Main results:
To measure the predictive skill, we use the anomaly correlation coefficient (ACC) metric. In addition, to quantify the impact of SIC assimilation on the predictive skill, we compute ACC differences between the system initialised with the enhanced reconstruction and the system initialised from the baseline reconstruction. Figure 3.8.2 shows that SIC assimilation provides clear improvements in the prediction of SIC that are visible in the first forecast month (May), in particular over the Atlantic sector of the Arctic, and persist in June and also July-August-September, when important increases in skill are visible in the Barents Sea.

Interestingly, skill improvements with SIC assimilation are also seen beyond the Arctic. The most striking improvement is a region of increased ACC in SST in the North Atlantic. The improvements start emerging during May and intensify over the subsequent months (Figure 3.8.3 top row). The initial improvement in May appears to be connected with the SIC improvements, via a teleconnection mechanism between Arctic Sea Ice and the atmospheric circulation in the North Atlantic (not shown), which leads to a local improvement in the predictability of the geopotential height at 500m (GPH500; Figure 3.8.3 bottom row). This improved skill in GPH500 leads to improved predictions of the local surface atmosphere temperature, which can explain the SST improvements (Figure 3.8.3 middle row). Persistence mechanisms in the ocean amplify and maintain the skill improvements in North Atlantic SSTs at subsequent forecast months.

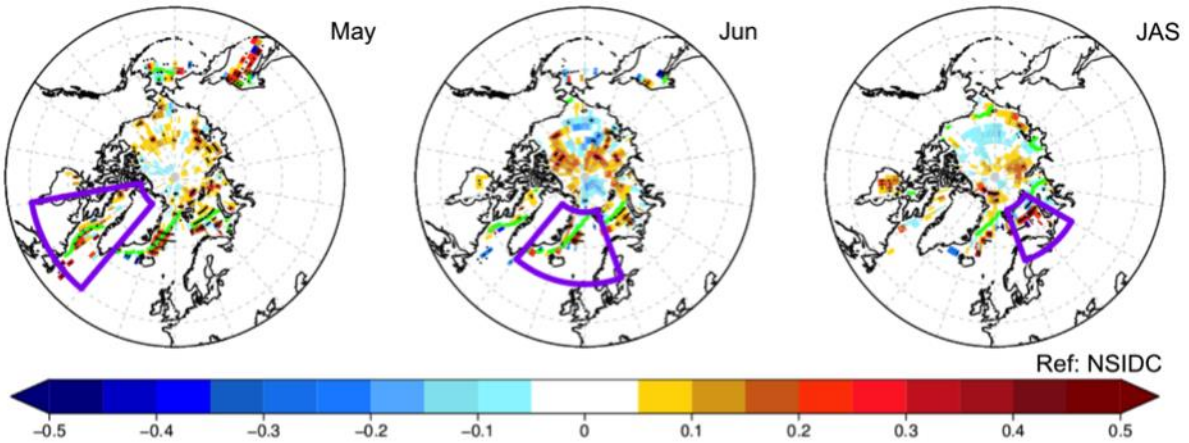

Figure 3.8.2: *Difference in the Anomaly Correlation Coefficient (ACC) for predicting the Sea Ice Concentration in May (left), June (center) and July-August-September (right) between two sets of seasonal re-forecasts, one initialised from the enhanced reconstruction and another from the baseline reconstruction. Positive values imply improved skill when SIC is assimilated. Both re-forecast systems include 30 members and cover the period 1992-2018. ACC values are computed against the observational reference NSIDC, which is independent from those considered for assimilation. Significant differences at the 95% confidence level are highlighted with stippling.*

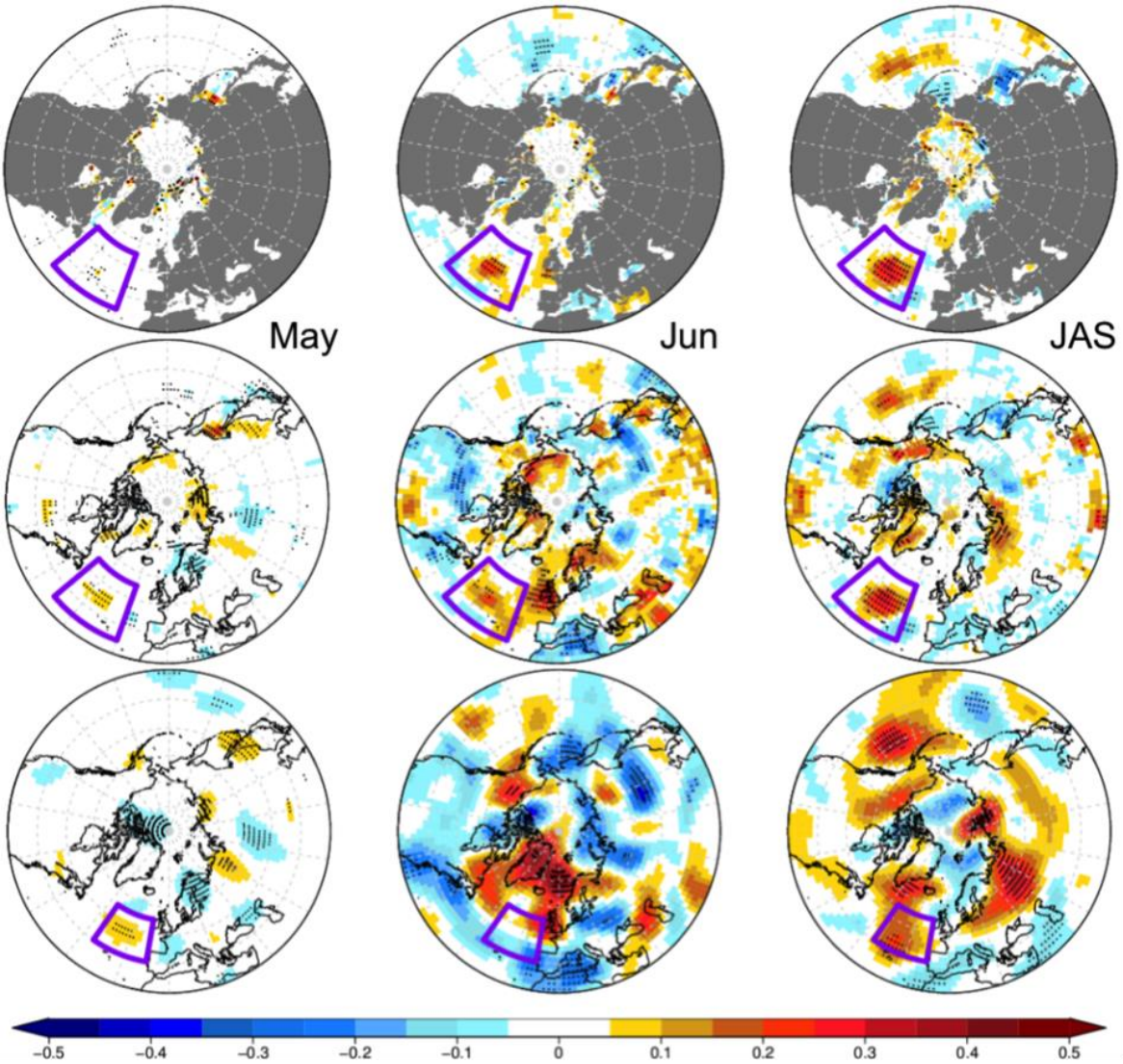

Figure 3.8.3: *The same as in Figure 3.8.2 but for the ACC differences in sea surface temperature (top), 2m air temperature (middle) and the geopotential height at 500m (bottom). In all cases the reference observational dataset is ERA5.*

The SST improvements have a beneficial impact on the predictability of the atmospheric circulation during the late summer and autumn (Figure 3.8.4 top row). This role of the SST is further supported by the ACC difference maps in the bottom panels of Figure 3.8.4. in which the reforecast system initialised with SIC assimilation is compared against itself, but after regressing out, from the forecasted GPH500, the variability of an SST index averaged over the North Atlantic region of the skill improvements. This SST index is computed in July-August-September to represents a leading influence on the atmospheric circulation. The differences in the bottom panel of Figure 3.8.4 thus quantify the impact of those local SSTs on the predictive skill of GPH500 several months later, and nicely show that the largest impacts occur in the same regions in which the predictions with SIC assimilation have GPH500 predictive skill (Figure 3.8.4 top panel). Further analyses have shown that the skill improvements in GPH500 also translate into higher predictive skill for surface air temperature and precipitation over Eurasia (not shown).

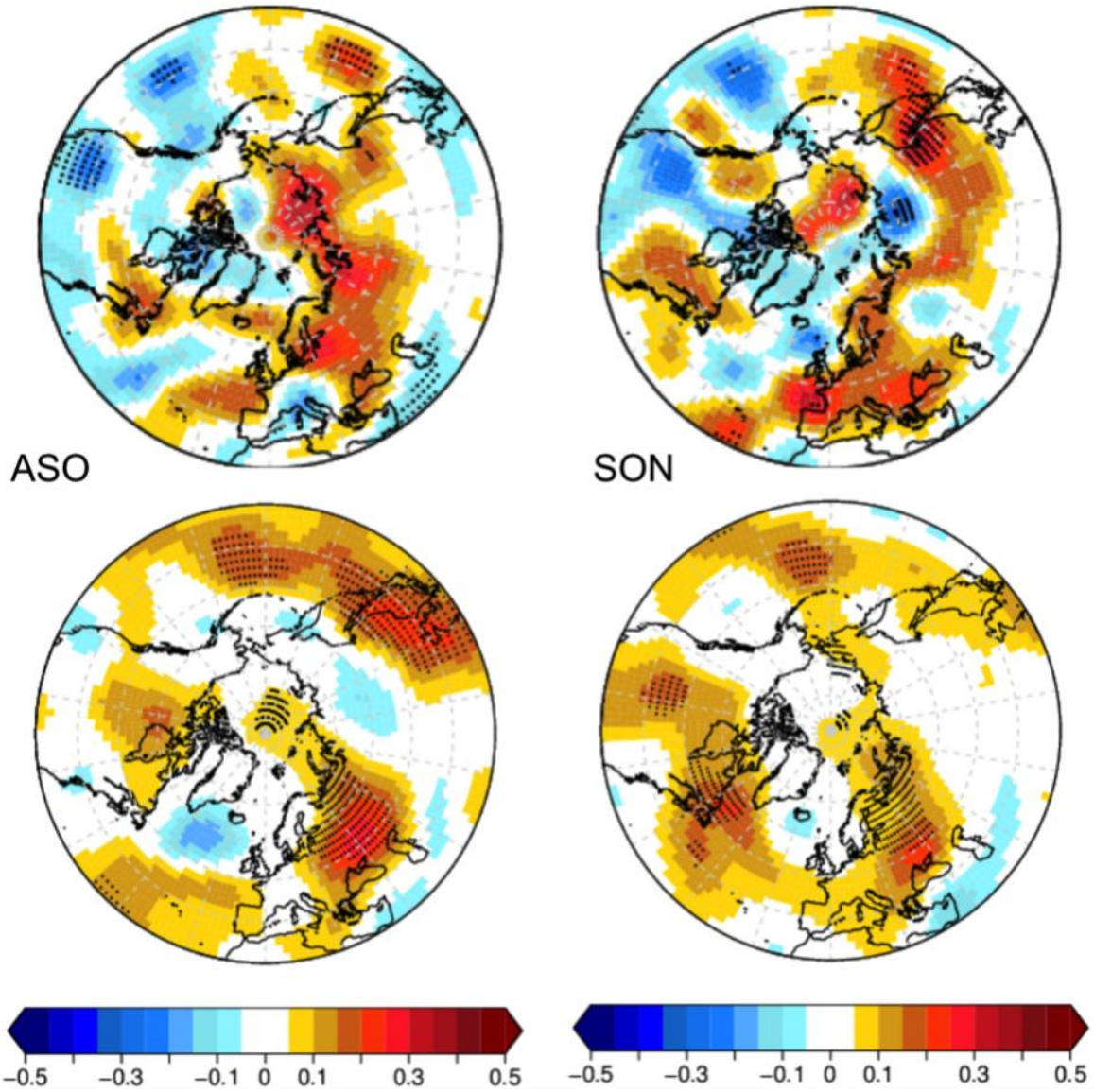

Figure 3.8.4: *(Top) ACC difference for the geopotential height at 500m in August-September-October (left) and September-October-November (right) in the two same reforecast systems of Figure 3.8.2. (Bottom) ACC difference between for the same variable and temporal averages, but in this case between the reforecast system initialised from the enhanced reanalysis, and the same system, but after regressing out the variability of SST in July-August-September averaged over a selected region in the North Atlantic (purple box in Figure 3.8.3 top panel).*

Publications

A scientific publication documenting the major results of this WP is currently under preparation, to be submitted to the journal Environmental Research Letters.

Interactions with the ECVs used in this experiment

There have been good interactions with the CCI ECV teams whose data are being used in this CMUG WP. In particular, Thomas Lavergne (Sea Ice CCI) recommended us the use of OSISAFv2as the most reliable product from the CCI on Sea Ice for the enhanced sea ice reanalysis.

Consistency between data products

We considered three different SIC products to produce the enhanced sea ice reanalysis to be able to explore the sensitivity of the results to the specific product used. No major differences have been observed. Figure 3.8.5 is included as an illustration of the large similarities across products. It shows the integrated ice edge error (a metric designed to measure the errors in predicting the sea ice edge that avoids error compensation) for the whole Arctic basin for three different cases. In each panel, only 10 members from the whole re-forecast system are considered, and correspond to all members that used either ORAS5, OSISAFv2 or CERSAT for assimilation. We can see that in all cases there are large error reductions in the first forecast month, followed by modest reductions in the second month (June). Those assimilating CERSAT seem to have also reduced errors in July, although is hard to tell if this result indicates that the CERSAT product is superior, or if this (and other) differences across products emerges due to the reduced number of members. We have also repeated some of the previous figures separately for the different members, and the main findings appear to be robust (e.g. the increased skill of SST in the North Atlantic with SIC assimilation, and the subsequent improvements in GPH500 skill).

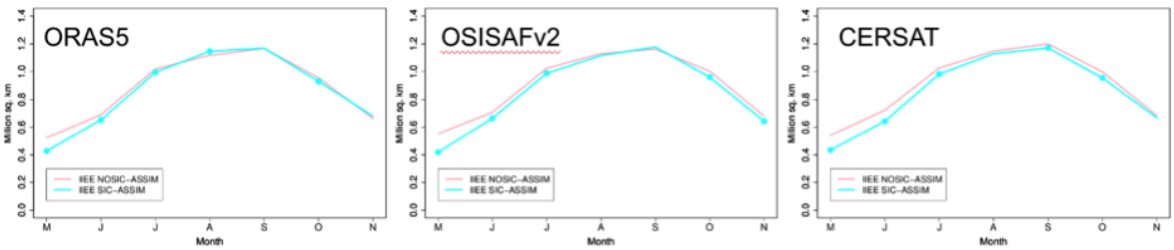

Figure 3.8.5: *Integrated Ice Edge Error as a function of forecast month in the re-forecast systems initialised from the enhanced and baseline reconstructions. Each panel shows the results for the members that are initialised assimilating one of the three different SIC datasets.*

Recommendations to the CCI ECV teams

To be completed in next version of this report.

Plan for Year 3

So far only the SIC data assimilated in WP3.8 comes from the ESA CCI program. We plan to use SST and SSS for the skill assessment, but that will be done in the final deliverable.
During the final months of CMUG we will devote our efforts to write a scientific publication documenting the previous results.

3.9 Biophysical feedbacks in the global ocean

Lead partner: Met Office
Authors: David Ford

Aim

The distribution of chlorophyll in the ocean has an impact on light attenuation and therefore ocean heat uptake, changing the ocean physics and sea ice. However, this biophysical feedback is not yet commonly included in climate models or reanalyses. This activity will assess the suitability of CCI ocean colour products to constrain this process when assimilated into coupled physical-biogeochemical ocean reanalyses. Assimilating ocean colour data has been demonstrated to improve the accuracy of 3D model chlorophyll, and it is expected that this will lead to more accurate simulation of light attenuation and ocean heat uptake in reanalyses, when biophysical feedback processes are included. This should then improve consistency with other ECVs. Furthermore, air-sea CO_2 flux parameterisations typically used in climate models do not use sea surface state as an input, even though this is known to play a role. A further experiment will assess the impact on air-sea gas exchange of including sea state data as an input in the flux parameterisation. It will address the following scientific questions:

1. Two equivalent reanalyses will be performed with NEMO-CICE-MEDUSA, assimilating CCI ocean colour products, and spanning a period of variability in the El Niño Southern Oscillation (ENSO), in which biophysical feedbacks are known to play a role. The first reanalysis will have no feedback from biology to physics, as in standard climate models. The second reanalysis will include the process.
2. The two runs will then be assessed against CCI sea surface temperature (SST), sea level, sea surface salinity, and sea ice products, as well as in situ observations of temperature, salinity, carbon dioxide, and ocean heat content. This will assess the impact of including biophysical feedbacks, driven by assimilation of CCI ocean colour data, on the model representation of the physical ocean and cryosphere ECVs, the consistency of features between ECVs and processes, and the carbon cycle.
3. A further model run will include sea surface state data as an input to the model air-sea CO_2 flux parameterisation, and investigate the impact on the ocean carbon cycle compared with the standard parameterisation which just uses wind speed.

Key Outcomes of CMUG Research

1. Contact has been made with all marine ECV teams to discuss CMUG requirements, the details of the experiments, and which product releases will be most appropriate to use.
2. Precursor work has been performed which will directly inform the experiments.
3. ECV data has been downloaded and processed for input to the model observation operator.
4. The biophysical feedback process has been coded into the model, and reanalyses performed.

Summary of Results

The assimilation of chlorophyll from CCI ocean colour products to constrain the light attenuation and ocean physics builds on work previously performed with precursor GlobColour data, and during the previous phase of CMUG. A paper describing results assessing multivariate consistency of ocean CCI products, from experiments performed during the previous phase of CMUG, has recently been published in a peer-review journal (Ford, 2020, "Assessing the role and consistency of satellite observation products in global physical-biogeochemical ocean reanalysis", https://os.copernicus.org/articles/16/875/2020/). This was followed up by a blog post for EGU highlighting CCI and CMUG (https://blogs.egu.eu/divisions/os/2020/09/22/satellite-data-for-ocean-reanalysis/).

A key result from this paper, which will directly inform the work performed in WP3.9, is shown in Fig. 3.9.1. Previous studies have suggested a direct correlation between the timing of the initiation of the spring bloom and that of the annual switch from negative to positive air-sea heat fluxes. Other studies have reached contrasting or mixed conclusions. This may in part be due to some studies looking at chlorophyll concentration, and others at phytoplankton biomass. The reanalyses produced as part of CMUG provided an opportunity to look at this relationship in a long model time series, and the impact of data assimilation. In the free-running model, there was a strong positive correlation between phytoplankton biomass and net air-sea heat flux across much of the ocean, whereas for chlorophyll concentration the correlation with net air-sea heat flux was weaker, and often negative at low latitudes. This suggests that seasonal variations in carbon-to-chlorophyll ratio play an important role, and that studies of phytoplankton bloom initiation based solely on chlorophyll data may not provide a full understanding of the underlying processes.

In WP3.9, chlorophyll derived from ocean colour will be assimilated, constraining the model chlorophyll, and with the addition of a feedback on the light attenuation, which will then affect the air-sea heat fluxes. This will provide the opportunity to study the two-way coupling between air-sea heat fluxes and timing of phytoplankton blooms, and it is envisaged that this will lead to a publication in a peer-reviewed journal.

Following discussion with the ECV teams, the v4.2 ocean colour release is being used for assimilation, and the v2.1 SST, v1.8 salinity, and v2.0 sea level products for validation. For sea ice concentration, only OSI SAF products provide a gap-free record of the period under consideration. These products have all been downloaded and processed for use in the model observation operator code, allowing model-observation match-ups to be computed in observation space while the model runs. More recent releases, including CCI sea ice concentration, could be used for later validation of monthly mapped fields.

The biophysical feedback from chlorophyll to light attenuation has been coded up in the model, and thoroughly tested in low-resolution test runs with and without data assimilation. Higher resolution reanalyses at 1/4° resolution have been set running with and without the biophysical feedback turned on, and with and without ocean colour data assimilation. These runs are mostly complete, and assessment is ongoing.

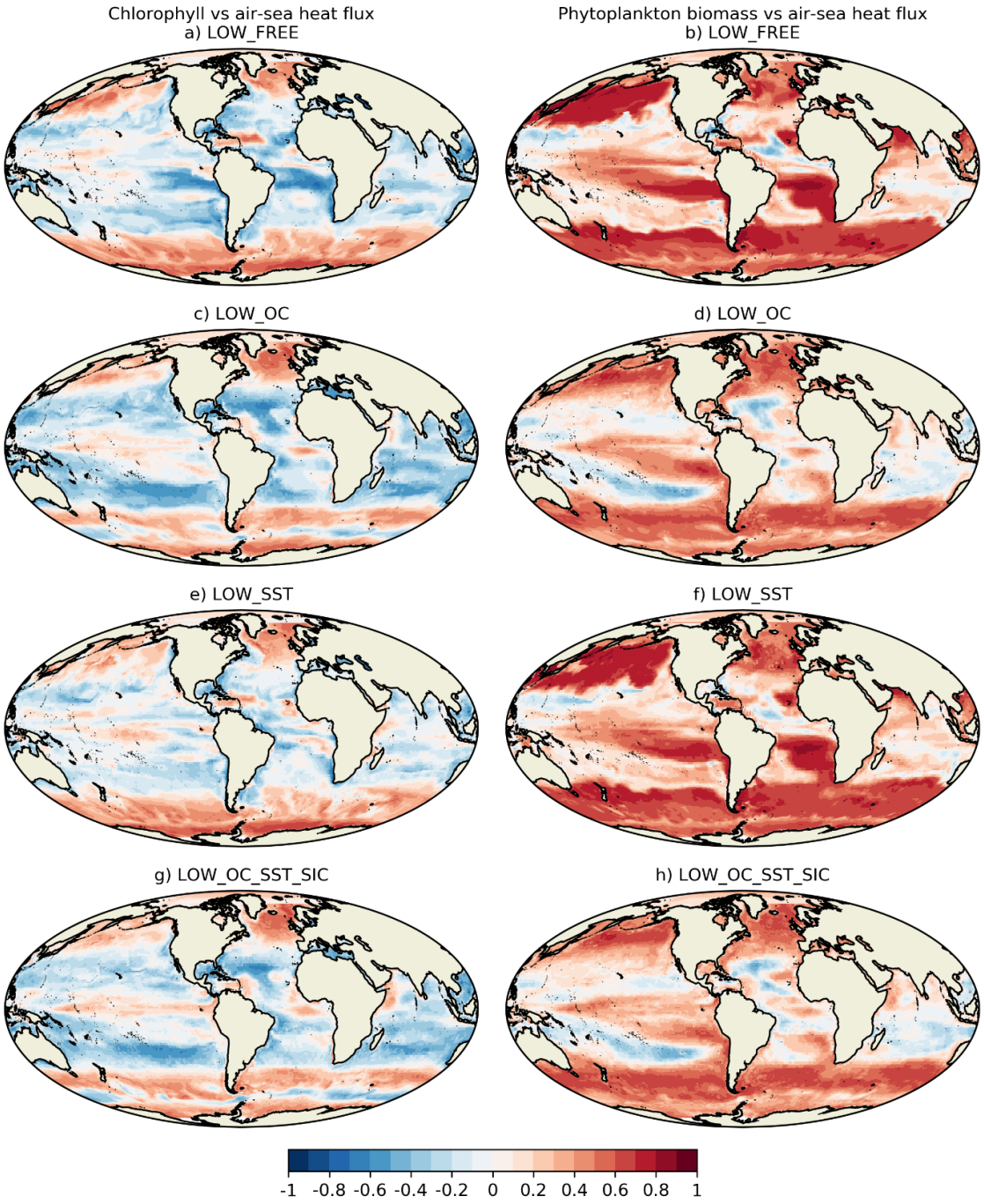

Figure 3.9.1*: Maps of correlation between surface chlorophyll and net air-sea heat flux (left column) and surface phytoplankton biomass and net air-sea heat flux (right column), covering 1998 - 2010 for model runs with (a-b) no data assimilation, (c-d) assimilation of CCI ocean colour, (e-f) assimilation of CCI SST, (g-h) assimilation of CCI ocean colour, SST and sea ice. Taken from Ford (2020).*

Publications

Ford, D. A.: Assessing the role and consistency of satellite observation products in global physical–biogeochemical ocean reanalysis, Ocean Sci., 16, 875–893, https://doi.org/10.5194/os-16-875-2020, 2020.

Interactions with the ECVs used in this experiment

There have been good interactions with the CCI ECV teams whose data are being used in this CMUG WP.

CMUG has had numerous interactions via email about user requirements and product availability with the marine ECV teams, as well as discussing the work with all relevant teams at the 2018 integration meeting, and reviewing the latest technical documents produced by the ocean colour, SST, sea state and sea level teams. Furthermore, plans and results were presented at a CSWG meeting in October 2020 focussing on SST, SSS and sea ice, with further discussion with the ECV teams present. CMUG also attended a SSS progress meeting in March 2021, and joint SSS-CMUG meeting in May 2021 to discuss working together.

Consistency between data products

In addition to relevant results described above, a record of any inconsistencies found between ECV products will be completed in this section in the next version of this report.

Recommendations to the CCI ECV teams

To be completed in next version of this report.

Plan for Year 3

During Year 3, the model runs testing the biophysical feedback will be completed and assessed, with a resultant journal paper planned if appropriate.

For the experiments using sea state, the most recent release will be used, with daily level 3 significant wave height data used in a model run as a sensitivity test to assess the potential impact of sea state on future reanalyses of air-sea CO_2 fluxes. This can then inform whether higher temporal resolution level 4 products are likely to be a future requirement or not, as this is currently unclear – it may be more appropriate to assimilate level 2 or level 3 products, or it may be that the impact on the model is small.

3.10 Assessment of the potential of CCI/CCI+ data to constrain mineral dust simulations at the regional scale

Lead partner: BSC
Authors: Enza Di Tomaso, Jeronimo Escribano, Carlos Pérez García-Pando

Aim

This contribution aims at demonstrating the use of CCI/CCI+ data to produce dust analyses at the regional scale. Part of its findings will set the basis for the assessment activity 3.11 on the production of a pilot dust reanalysis, where the impact on dust cycles at a seasonal scale will be evaluated.

Key Outcomes of CMUG Research

We have shown the benefit of assimilating IASI retrievals of dust optical depth (using pixel-level uncertainty) by assessing its impact at regional scale in high resolution simulations during a summer period that included an exceptional dust storm in the Eastern Mediterranean. We have shown that the assimilation of the IASI thermal infrared retrievals compares well with the assimilation of MODIS visible retrievals of (coarse) dust optical depth. The MODIS-based analysis, however, is better correlated with independent observations than the IASI-based analysis.

Summary of Results

The work done focused on the preparation of CCI aerosol data for the assimilation system, which included the processing of IASI dust aerosol data to follow the assimilation cycles, and the implementation of an observation operator for the thermal infrared. Assimilation experiments at high resolution were then performed over a regional domain involving relevant dust events.

Compared to a previous case study performed within the phase 2 of the aerosol_cci project, a more advanced assimilation of dust aerosol data was performed during this assessment activity with the aim of better demonstrating the use of CCI/CCI+ data to produce dust analyses at the regional scale. In particular the following novel aspects were introduced:

- Experiments were run on a regional scale to allow for high resolution simulations better representing the smaller features of dust events;
- Dust retrievals were assimilated at Level 2 resolution (circa 10 km) rather than Level 3 (1 degree) to avoid the propagation of observation uncertainties difficult to describe in a Level 3 product;
- Retrievals were assimilated at the original retrieval wavelength in the thermal infrared (10 μm) in order to avoid the introduction of errors due to the conversion to a different wavelength (e.g. in the visible part of the electromagnetic spectrum).

The preparation of the observations and of the assimilation system has involved three main tasks which have seen the contact with the Université Libre de Brussels's (ULB) retrieval team:

- IASI dust optical depth from Metop-A have been downloaded for the summer period of 2015. The period has been selected following the recommendation of the data providers: the most recent years of the IASI dust retrieval benefit of higher quality of the EUMETSAT ancillary data used in the retrieval algorithm.

- Retrievals have been filtered using the two flags provided (pre_quality_flag=1 and post_quality_flag=1). The pre-quality flag is set depending on cloud coverage (only cloud free data are processed), while the post-quality flag removes unreliable retrievals.

- The observation operator has been built for dust aerosol optical depth at 10 μm. The operator consists in calculating the model equivalent of the observations, i.e. to map the model background state vector into the observation space. Hence it has two components: the horizontal interpolation component (model tracers are interpolated at the observation location), followed by the calculation of a total column extinction from a model mass concentration profile.

The extinction efficiency factors for 10 μm used in the latter calculation were estimated using the Mie scattering theory assuming dust spherical, non-soluble particles for the 8 model size bins, and, within a bin, a lognormal distribution for dust with geometric radius of 0.2986 μm and standard deviation of 2.0. Information on refractive indices was taken from results of an experimental campaign rather than from the more commonly used OPAC database.

High resolution assimilation experiments over a regional domain including Northern Africa, the Middle East and Europe were performed at a 0.1° latitude × 0.1° longitude horizontal resolution and 40 hybrid pressure-sigma model layers. This domain configuration is used operationally to deliver daily forecasts at the World Meteorological Organisation Barcelona Dust Regional Center (https://dust.aemet.es/). IASI analyses were produced using Local Ensemble Transform Kalman Filter (LETKF) data assimilation in the Multiscale Online Non-hydrostatic AtmospheRe CHemistry model (MONARCH) developed at the Barcelona Supercomputing Center (BSC). We have applied spatial covariance localization by which the influence of an observation on the analysis decays gradually toward zero as the distance from the analysis location increases. The localization factor was set such that the observation influence practically fades to zero before 30 model grid points away from the observation location (in the horizontal plane).

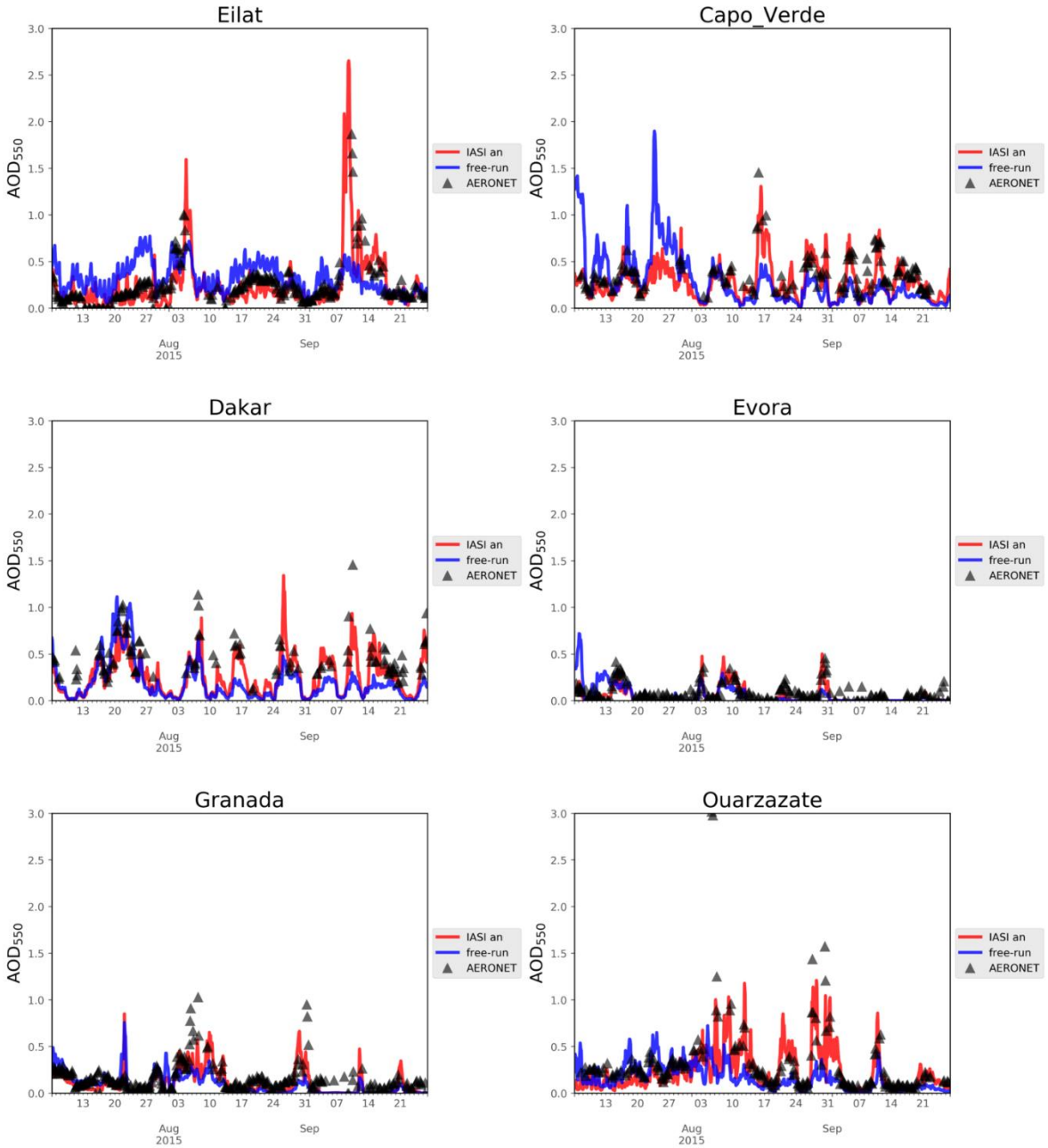

Figure 3.10.1*: Time series of the dust AOD from the IASI analysis (red), the free-run simulation (blue) and independent ground-based observations (AERONET direct sun; black triangles) for summer of 2015 at Eilat (Israel), Capo Verde (right), Dakar (Senegal), Evora (Portugal), Granada (Spain) and Ouarzazate (Morocco).*

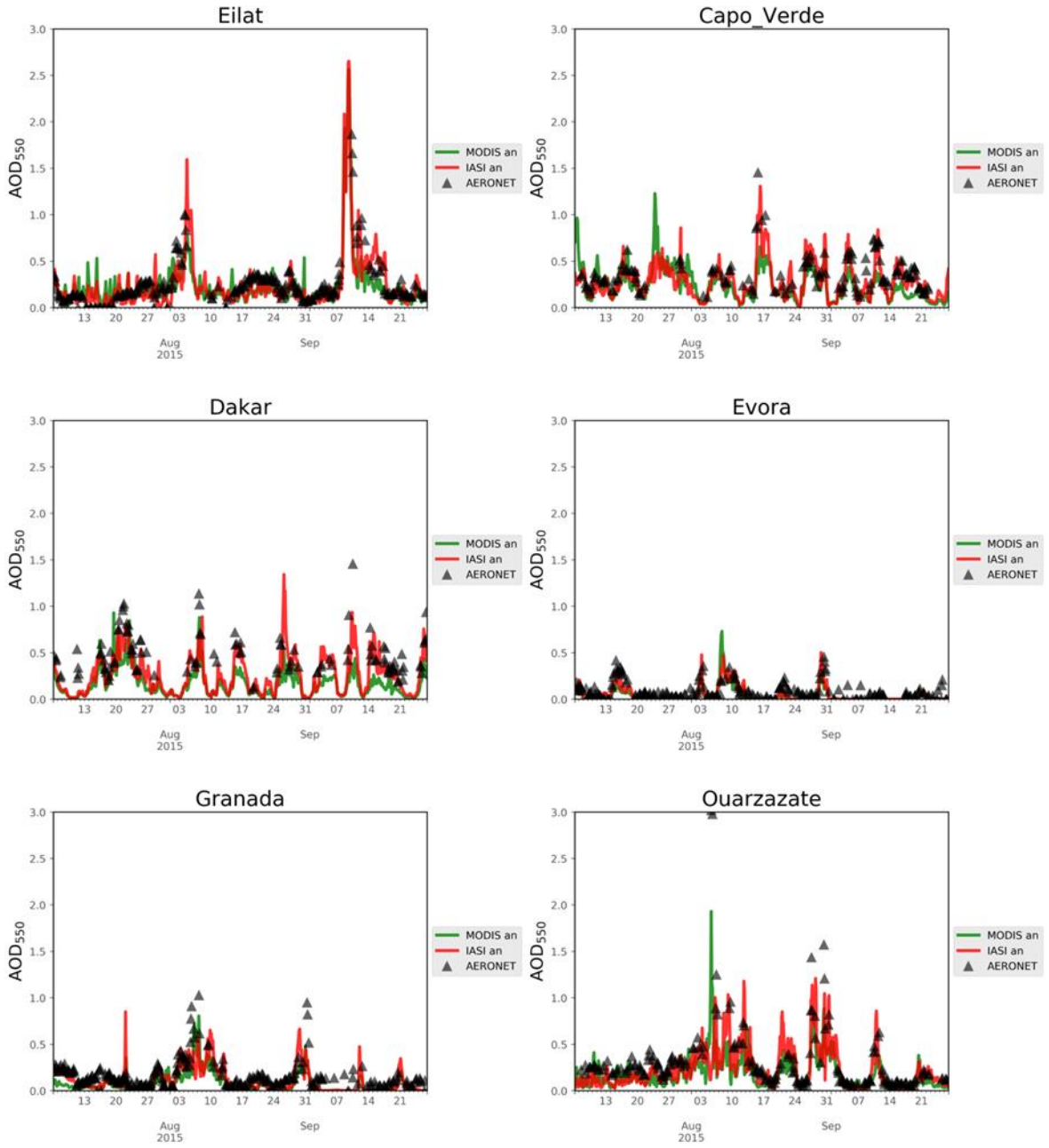

Figure 3.10.2*: Timeseries of dust AOD from the IASI analysis (red), the MODIS analysis (green) and independent ground-based observations (AERONET direct sun; black triangles) for summer of 2015 at Eilat (Israel), Capo Verde (right), Dakar (Senegal), Evora (Portugal), Granada (Spain) and Ouarzazate (Morocco).*

The control variable is formulated in terms of the total mixing ratio over the 8 model prognostic variables (corresponding to different dust particle size bins) used to simulate the transport of dust in MONARCH. After the estimation of total dust mixing ratio analysis, the analysis increments are partitioned among the dust size bin according to their fractional contribution to the total mixing ratio

in the forecast step. Figure 3.10.1 shows the IASI analysis for dust Aerosol Optical Depth (AOD) at 550 nm during a summer period in 2015 together with a free-run simulation (an ensemble simulation with no data assimilation) and with AERONET dust-filtered AOD values from the direct-sun algorithm (version 2, level 2.0) at 6 different locations. While the intensity of some events is underestimated by the IASI analysis, there is a general good agreement between the analysis simulation and the observations in the identification of the dust events both in the short- and long-range dust transport. The study period includes a remarkable dust event that occurred in the Eastern Mediterranean between the 6th and 13th of September 2015 that is well described by the IASI analysis at the Eilat AERONET station in Israel. Figure 3.10.2 shows that the IASI analysis compares well with a MODIS-based analysis produced by BSC with similar settings and resolution than the IASI analysis, with some of the dust events, for example in Granada (Spain) or Capo Verde, better depicted in one or the other analysis. Some of the differences between the two analyses might be due to a different coverage of the IASI and MODIS retrievals. Preliminary verification statistics show a higher correlation of the MODIS analysis (r=0.82) than the IASI analysis (r=0.76) with the AERONET observations shown in Figure 3.10.2 and a comparable root mean square error (RMSE=0.2).

Publications

None so far, but the interest in the results leading to a journal or conference publication will be described in the next version of this report.

Interactions with the ECVs used in this experiment

There have been interactions with Lieven Clarisse (who was involved in Aerosol_cci during CCI Phase 2) from the Université Libre de Brussels (ULB) on the IASI dust aerosol retrievals.

Consistency between data products

This section will provide a record of any inconsistencies found between ECV products, and will be completed in the next version of this report.

Recommendations to the CCI ECV teams

To be completed in next version of this report.

Plan for Year 3

Plans for Year 3 involve consolidating the evaluation of the IASI analysis with the inclusion of the comparison against the AERONET SDA (Spectral Deconvolution Algorithm) coarse mode product and investigating whether the CCI Land Cover product can improve MONARCH simulations.

3.11 Production of a pilot dust reanalysis at the regional scale

Lead partner: BSC
Authors: Enza Di Tomaso, Jeronimo Escribano, Carlos Pérez García-Pando, Oriol Jorba

Aim

This contribution aims at producing a pilot dust reanalysis based on CCI/CCI+ data, and at assessing whether their integration in model simulations can improve the monitoring of mineral dust and the characterization of dust cycles.

Key Outcomes of CMUG Research

1. A pilot IASI reanalysis for 1 year (2015) has been produced for a regional domain and at a high spatial resolution;
2. Some of the main features of the dust seasonal cycle are well represented by the IASI analysis during the year considered. However, dust concentrations in the winter months are particularly low when assimilating IASI dust retrievals;
3. The comparison with a MODIS-based reanalysis produced at the same spatial resolution showed that the IASI retrievals weaken the analysis of dust optical depth over some major emission areas;
4. The consistency of the assimilation procedure has been proven by the analysis of simulation departures from assimilated observations.

Summary of Results

This assessment activity is based on the results of the assessment activity 3.10 on the potential of CCI/CCI+ data to constrain mineral dust simulations at the regional scale. Initially, preparatory technical work was necessary on the refinement of the BSC technical infrastructure for high resolution (computationally demanding) IASI assimilation experiments to be run over a regional domain and over the longer (1 year) period of the pilot dust reanalysis, compared to what it is planned for selected dust events in 3.10. As part of this work, advances have been made in the BSC simulation workflow manager in order to improve the automatization of experiments and to optimize the storage of simulations' outputs. Subsequently, the assimilation of IASI dust Level 2 into a high-resolution regional simulation (0.1 x 0.1°) for a full year has been performed to produce a pilot study for an IASI dust reanalysis.

Deviation of plans: the pilot reanalysis is finally based on a dust aerosol CCI product with no use of CCI+ land cover information since high resolution land cover (HRLC) data was not available for this run. The production of a pilot reanalysis at high resolution and with an ensemble-based data assimilation is a computationally intensive task that had to be performed at a specific stage in the workflow with the available computational resources. Given its restricted spatial availability on a small portion of the domain of interest, the HRLC would have been likely of a very minor impact on the reanalysis. The main features of the dust seasonal cycle are well represented by the IASI analysis and first-guess of Dust Optical Depth (DOD) as shown in Figure 3.11.1 (left and central column): for example, the mobilization of dust in the Taklamakan region in spring and in the Arabian peninsula

during summer, the transport of south Saharan dust south-west toward the Gulf of Guinea during winter and spring, the shift toward northern latitudes of the plume originated in Western Africa and transported across the tropical Atlantic during summer, or low dust optical depth simulated everywhere in autumn. The lowest values of dust optical depth of the IASI analysis occur in the winter months, which deserve some further attention due to less accurate IASI dust retrievals in that season, as confirmed by the retrieval team. The analysis increments in Figure 3.11.1 (right column) show the impact of the observations, indicating the correction of some systematic overestimation (blue; in particular over emission source areas) or underestimation (red) of dust concentrations according to the IASI dust retrievals.

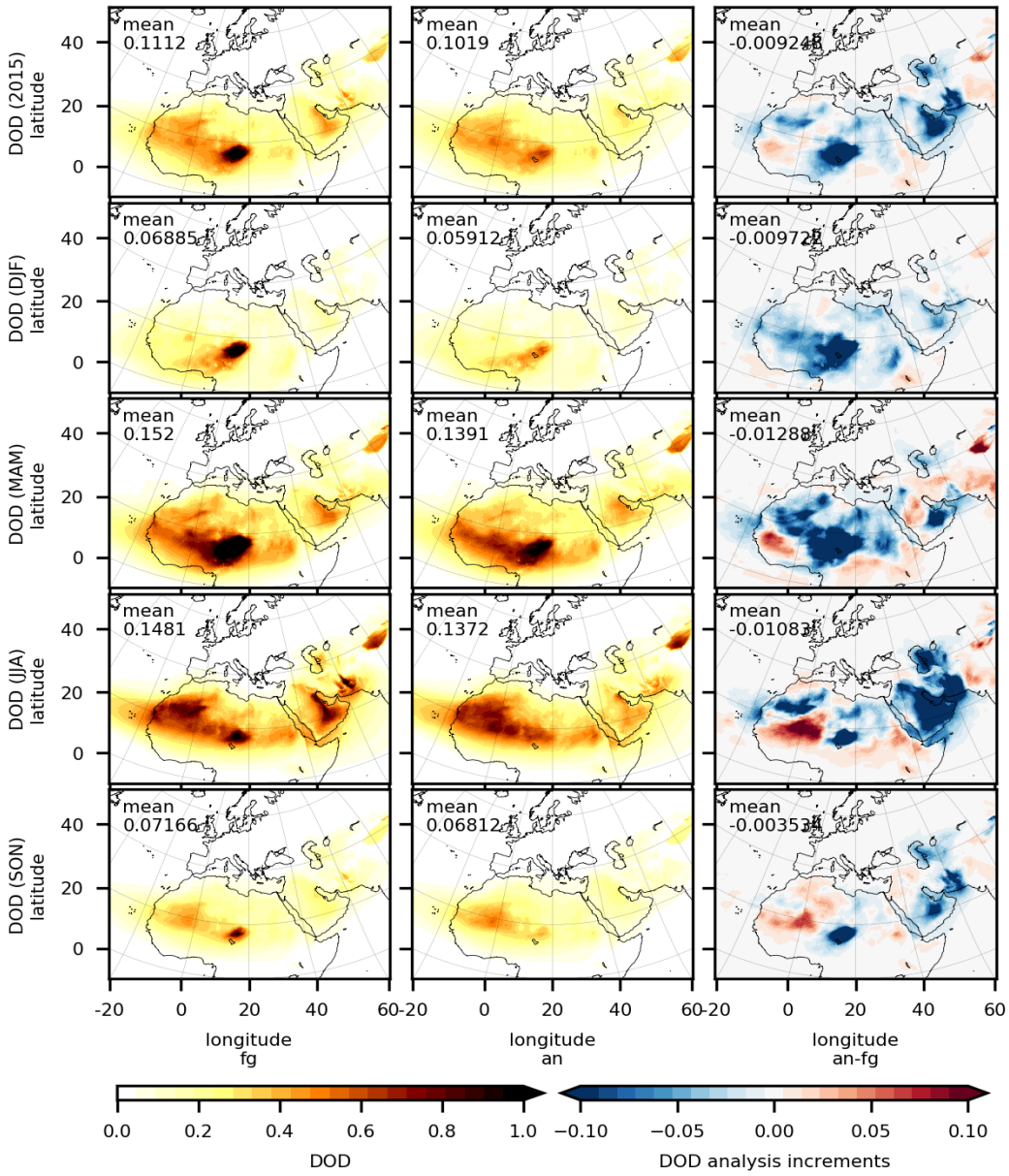

Figure 3.11.1: ***Maps of first-guess simulations (left), IASI analysis (centre) and their difference (analysis increments; right) averaged for 2015 (first raw) and for different seasons of that year (raw 2 to 5).***

Figure 3.11.2 shows model simulation values (first-guess and analysis) collocated with the assimilated observations for IASI (DOD; top) and MODIS (DODcoarse; bottom). Retrievals (and consequently, analysis) of dust optical depth over the major emission areas of the domain, like the Bodélé depression in Chad and the Arabian desert, are considerably lower for IASI than MODIS. This might be due to IASI observations being less sensitive to surface layers of dust, as confirmed by the retrieval team.

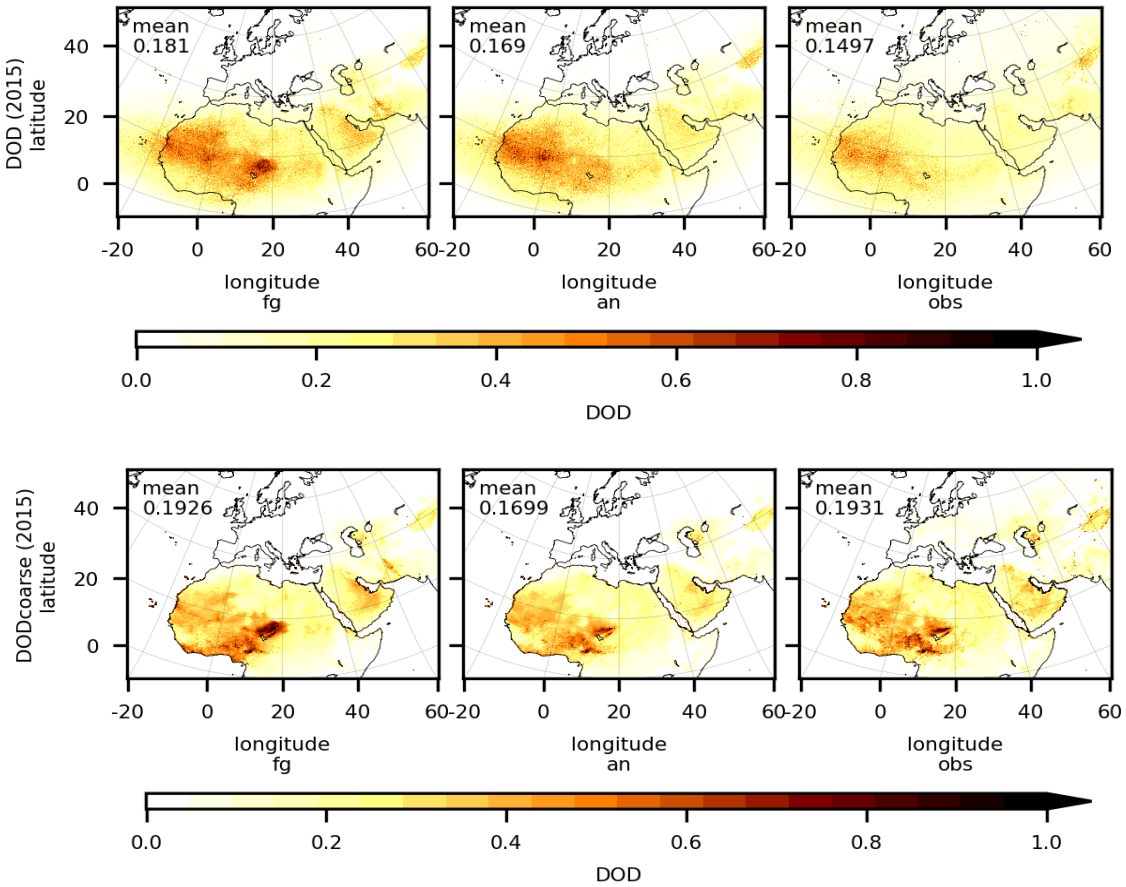

Figure 3.11.2*: Collocated values of Dust Optical Depth (DOD) for IASI first-guess, analysis and observations (top), and collocated values of coarse Dust Optical Depth (DODcoarse) for MODIS first-guess, analysis and observations (bottom).*

Figure 3.11.3 shows that bias and standard deviation of departures from assimilated IASI observations calculated for the whole year of 2015 are reduced in the analysis compared to the first-guess, proving the consistency of our assimilation procedure.

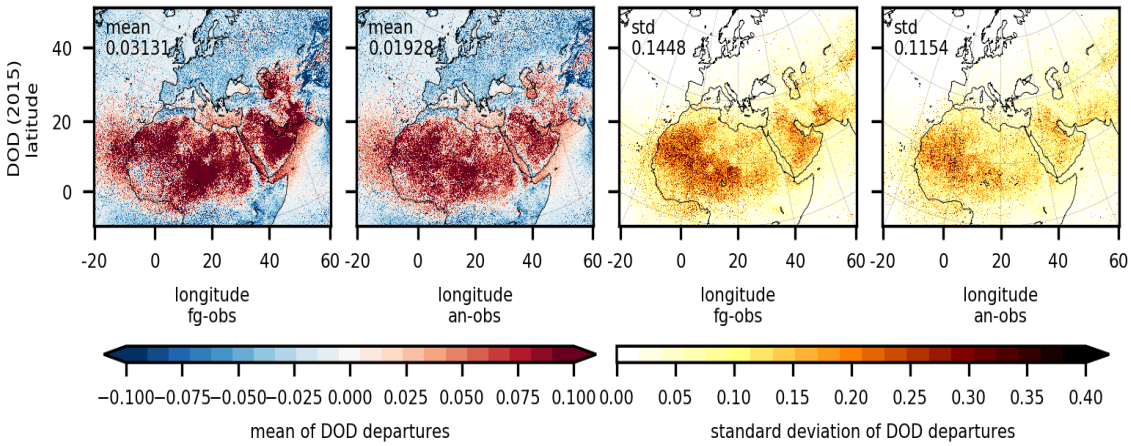

***Figure 3.11.3**: Bias and standard deviation of the departures of IASI assimilated observations from first-guess and analysis.*

Publications

None so far, but the interest in the results leading to a journal or conference publication will be described in the next version of this report.

Interactions with the ECVs used in this experiment

There have been interactions with Lieven Clarisse (formerly a partner in the CCI Phase 2 Aerosol project) from the Université Libre de Brussels (ULB) on the IASI dust aerosol retrievals.

Consistency between data products

This section will provide a record of any inconsistencies found between ECV products, and will be completed in the next version of this report.

Recommendations to the CCI ECV teams

To be completed in next version of this report.

Plan for Year 3

Next, we will complete the verification with independent observations (AERONET) for the full period of study and calculate the commonly used validation statistics (correlation, bias, RMSE) to assess the overall quality of the IASI pilot reanalysis.

3.12 Integrated assimilation of the CCI+ Sentinel 3 AOD and Sentinel 5P ozone retrievals in the IFS

Lead partner: ECMWF
Authors: Rossana Dragani, Angela Benedetti

Aim

The aim of this research is to assess the impact of assimilating the CCI+ ozone retrievals from Sentinel 5P (S5P) and Aerosol Optical Depth (AOD) from the Sentinel 3 measurements to feed back to the Copernicus Climate Change Service (C3S) and Copernicus Atmosphere Monitoring Service (CAMS) reanalyses. It will address the following scientific questions:

1. Are the CCI+ ozone and aerosol data suitable for constraining a global reanalysis?
2. Assessment of the uncertainty characteristics provided with the CCI data using the ECMWF data assimilation system
3. Assess consistency between the two CCI data records via a data assimilation system and with independent observations
4. Assess consistency of the produced reanalysis with existing global reanalyses.

Summary of Work

S3 SLSTR AOD experiments

The assimilation experiments using the latest release of the SU SLSTR AOD product (v1.14) in the Integrated Forecast System in composition configuration used by CAMS, have been completed. A full report has been submitted to ESA via the AER CCI+ team, under which funding the work was completed. A key result of the study was to show the positive impact of the SLSTR data with respect to a run with no aerosol data assimilation. However, the best configuration as compared to the independent AERONET AOD dataset is still the one which uses MODIS and PMAP AODs in addition to the SLSTR data.

S5P TCO3 experiments

Experiments were run over the period September-December 2020 to understand the impact of the CCI S5P Tropomi TCO3 (Total Column Ozone) observations provided by DLR (German Aerospace Centre) using the retrieval of BIRA (Belgian Institute for Space Aeronomy) on the NWP configuration of the Integrated Forecast System. This CCI S5P Tropomi TCO3 dataset is from collection 1 of September 2020 with processor version 02.01.03 for both near real time (NRTI) and offline (OFL) versions.

More specifically, the following products were used:

- NRTI data 01_020103 from 01/09/2020 until 02/12/2020
- NRTI data 01_020104 from 02/12/2020 until 30/12/2020

for the runs with the NRT product and

- OFL data 01_020103 from 12/07/2020 until 29/11/2020

for the runs with the offline product.

The analysis of the experiments shows a small but tangible impact of using the Sentinel5P (S5P) TROPOMI total column O_3 (TCO3) data on the NWP performance. A comparison of one-month assimilation experiments with the CCI+ S5P offline TCO3 product and the near real-time (NRT) TCO3 product shows that the performance of the NRT product is slightly better for certain aspects and slightly worse for others. Longer experiments might be needed to be able to come to a firmer conclusion. Overall, there is no adverse impact of using the S5P TCO3 data in the NWP and it has been recommended to start using this dataset in the NWP operational configuration as it is done in the CAMS configuration.

This research has benefitted from the work performed within CAMS by Antje Inness and Roberto Ribas who are gratefully acknowledged. In particular, due to the high resolution of the S5P data, a preprocessing called *superobbing* has been put in place in order to be able to exploit these observations at the resolution of the analysis.

Some results are shown in the figures below. Standard scores show a small but positive (and statistically significant) impact on the NWP resulting in a reduction of root mean square error for upper-level geopotential in the experiment with active S5P (NRT) data at day 1 (T+24) and day 2(T+48). A slight degradation is observed at T+12.

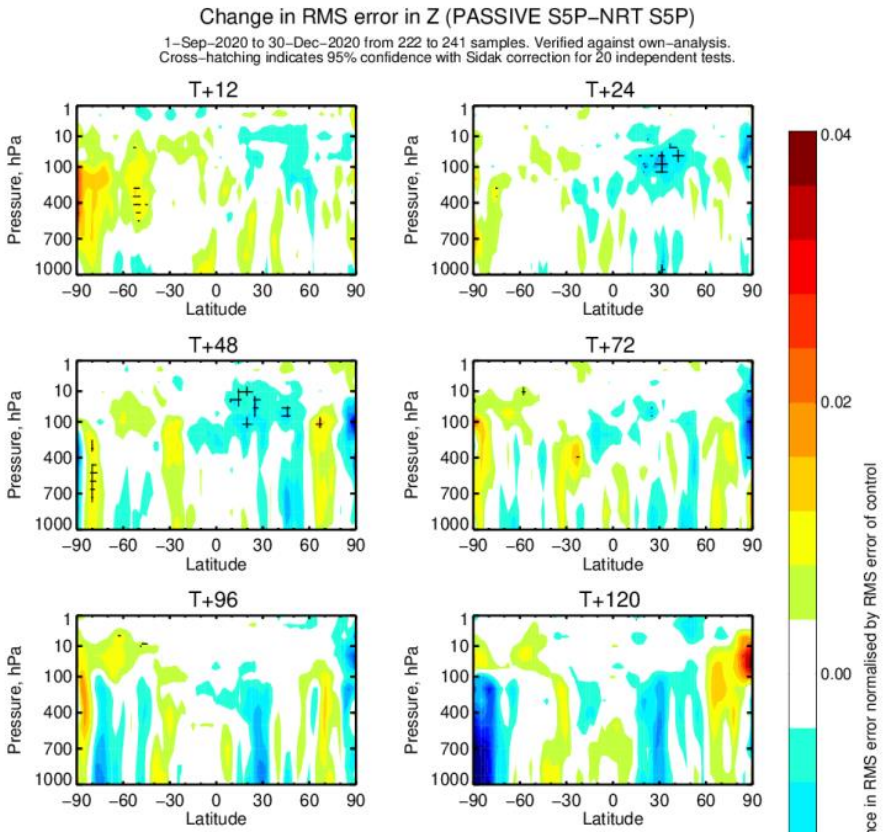

Figure 3.12.1*: Change in RMS error in geopotential for the experiment with passive S5P data compared to active S5P TCO3 data. Blue indicates a reduction in RMSE. Hatched areas are statistically significant at the 95% level.*

When looking at independent observations, particularly the infrared hyperspectral instruments, it is possible to see the role of the S53 TCO3 in improving the fit to the radiance observations at upper levels. The improvement is mainly due to the Tropics with up to a 4% higher standard deviation in the experiments without S5P TCO3.

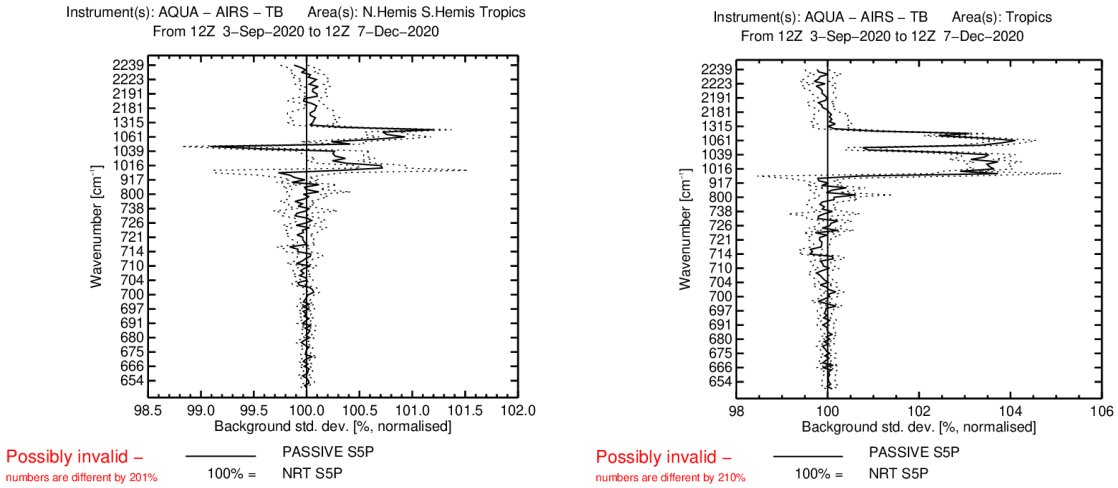

Figure 3.12.2*: Standard deviation of passive S5P TCO3 experiment with respect to NRT S5P TCO3 assimilation experiment (represented by the vertical 100% line). Note the increase of the std deviation at upper levels, particularly at the Tropics in the experiment without S5P TCO3 data.*

Similar plots were analyzed for the experiments with the offline S5P TCO3 CCI+ datasets for the month of September 2020. The impact of the offline dataset seems to be less positive than that of the NRT datasets (picture not show). It might be due to the fact that only one month of data were used and a longer period is needed to come to final conclusions regarding the relative merits of the offline versus the NRT S5P TCO3 dataset.

Publications

None so far, but the interest in the results leading to a journal or conference publication will be described in the next version of this report.

Interactions with the ECVs used in this experiment

In the first 12 months of this phase of CMUG work there have been interactions with the Aerosol and Ozone CCI ECV teams at the quarterly CSWG meetings and the Integration meetings and by personal contact, attendance at an ECV project meeting, and email.

Consistency between data products

This section will provide a record of any inconsistencies found between ECV products, and will be completed in the next version of this report.

Recommendations to the CCI ECV teams

To be completed in next version of this report.

Plan for Year 3

The plan for Year 3 is to finalize the analysis of the ozone and aerosol experiments with the view to provide feedback to the CCI+ teams regarding the quality of the datasets for reanalysis purposes.

4. References

Acosta-Navarro JC, Ortega P, García-Serrano J, et al (2019) December 2016: Linking the Lowest Arctic Sea-Ice Extent on Record with the Lowest European Precipitation Event on Record. Bull Am Meteorol Soc 100:S43–S48. doi: 10.1175/BAMS-D-18-0097.1

Ait-Mesbah,S. F. Cheruy , J.L. Dufresne F. Hourdin, On the representation of surface temperature in semi-arid and arid regions, Geophys. Res. Lett., 42(18), pp. 7572–7580, 2015, doi:10.1002/2015GL065553.

Bellprat, O., F. Massonnet, S. Siegert, C. Prodhomme, D. Macias-Gómez, V. Guemas, F. Doblas-Reyes (2017) Uncertainty propagation in observational references to climate model scales. Remote Sensing of Environment. Volume 203, 15 December 2017, Pages 101-108. https://doi.org/10.1016/j.rse.2017.06.034.

Betts, A. K., Reid, D., & Crossett, C. (2020). Evaluation of the FLake Model in ERA5 for Lake Champlain. *Frontiers in Environmental Science*, *8*. https://doi.org/10.3389/fenvs.2020.609254

Cheruy F., A. Ducharne, F. Hourdin, I. Musat, G. Gastineau, E. Vignon et al. 2020 : Improved near surface continental climate in IPSL-CM6 by combined evolutions of atmospheric and land surface physics, submitted to JAMES, Dec. 2019.

Cornes, R. C., van der Schrier, G., van den Besselaar, E. J. M., & Jones, P. D. (2018). An Ensemble Version of the E-OBS Temperature and Precipitation Data Sets. *Journal of Geophysical Research: Atmospheres*, *123*(17), 9391–9409. https://doi.org/10.1029/2017JD028200

Dee, D. P., Uppala, S. M., Simmons, A. J., Berrisford, P., Poli, P., Kobayashi, S., Andrae, U., Balmaseda, M. A., Balsamo, G., Bauer, P., Bechtold, P., Beljaars, A. C. M., van de Berg, L., Bidlot, J., Bormann, N., Delsol, C., Dragani, R., Fuentes, M., Geer, A. J., … Vitart, F. (2011). The ERA-Interim reanalysis: configuration and performance of the data assimilation system. *Quarterly Journal of the Royal Meteorological Society*, *137*(656), 553–597. https://doi.org/10.1002/qj.828

Gordon, H. B.; Rotstayn, L. D.; McGregor, J. L.; Dix, M. R.; Kowalczyk, E. A.; O'Farrell, S. P.; Waterman, L. J.; Hirst, A. C.; Wilson, S. G.; Collier, M. A.; Watterson, I. G.; Elliott, T. I. (2002). The CSIRO Mk3 Climate System Model. *Aspendale: CSIRO Atmospheric Research*. https://doi.org/https://doi.org/10.4225/08/585974a670e09

Jacob, D., Petersen, J., Eggert, B., Alias, A., Christensen, O. B., Bouwer, L. M., Braun, A., Colette, A., Déqué, M., Georgievski, G., Georgopoulou, E., Gobiet, A., Menut, L., Nikulin, G., Haensler, A., Hempelmann, N., Jones, C., Keuler, K., Kovats, S, P. (2014). EURO-CORDEX: New high-resolution climate change projections for European impact research. *Regional Environmental Change, 14(2), 563–578*. https://doi.org/https://doi.org/10.1007/s10113-013-0499

Kotlarski, S., Keuler, K., Christensen, O. B., Colette, A., Déqué, M., Gobiet, A., Goergen, K., Jacob, D., Lüthi, D., van Meijgaard, E., Nikulin, G., Schär, C., Teichmann, C., Vautard, R., Warrach-Sagi, K., & Wulfmeyer, V. (2014). Regional climate modeling on European scales: a joint standard evaluation of the EURO-CORDEX RCM ensembleNo Title. *Geoscientific Model Development*, *7(4)*, *1297–1333*. https://doi.org/https://doi.org/10.5194/gmd-7-1297-2014

Kotlarski, S., Szabó, P., Herrera, S., Räty, O., Keuler, K., Soares, P. M., Cardoso, R. M., Bosshard, T., Pagé, C., Boberg, F., Gutiérrez, J. M., Isotta, F. A., Jaczewski, A., Kreienkamp, F., Liniger, M. A., Lussana, C., & Pianko-Kluczyńska, K. (2019). Observational uncertainty and regional climate model evaluation: A pan-European perspective. *International Journal of Climatology*, *39*(9), 3730–3749. https://doi.org/10.1002/joc.5249

Layden, A., Merchant, C., & MacCallum, S. (2015). Global climatology of surface water temperatures of large lakes by remote sensing. *International Journal of Climatology*, *35*(15). https://doi.org/10.1002/joc.4299

MacCallum, S. N., & Merchant, C. J. (2012). Surface water temperature observations of large lakes by optimal estimation. *Canadian Journal of Remote Sensing*, *38*(1), 25–45. https://doi.org/10.5589/m12-010

Mallard, M. S., Nolte, C. G., Spero, T. L., Bullock, O. R., Alapaty, K., Herwehe, J. A., Gula, J., & Bowden, J. H. (2015). Technical challenges and solutions in representing lakes when using WRF in downscaling applications. *Geosci. Model Dev.*, *8*(4), 1085–1096. https://doi.org/10.5194/gmd-8-1085-2015

Merchant, C. J., Embury, O., Rayner, N. A., Berry, D. I., Corlett, G. K., Lean, K., Saunders, R. (2012). A 20 year independent record of sea surface temperature for climate from Along-Track Scanning Radiometers. *Journal of Geophysical Research*, *117*(C12), C12013. doi:10.1029/2012JC008400.

Rouse, W. R., Blanken, P. D., Duguay, C. R., Oswald, C. J., & Schertzer, W. M. (2008). Climate-Lake Interactions. In *Cold Region Atmospheric and Hydrologic Studies. The Mackenzie GEWEX Experience* (pp. 139–160). Springer Berlin Heidelberg. https://doi.org/10.1007/978-3-540-75136-6_8

Reynolds, R. W., Rayner, N. A., Smith, T. M., Stokes, D. C., Wang, W., Reynolds, R. W., Rayner, N. A., Smith, T. M., Stokes, D. C., & Wang, W. An Improved In Situ and Satellite SST Analysis for Climate. *Http://Dx.Doi.Org/10.1175/1520-0442(2002)015<1609:AIISAS>2.0.CO;2*. https://doi.org/10.1175/1520-0442(2002)015<1609:AIISAS>2.0.CO;2; 2002.

Ruggieri P, Buizza R, Visconti G (2016) On the link between Barents-Kara sea ice variability and European blocking. J Geophys Res Atmospheres 121:5664–5679. doi: 10.1002/2015JD024021.

Sevruk, B. (1985). Correction of precipitation measurements summary report. In: Correction of Precipitation Measurements. *Züricher Geographische Schriften, Vol. 23. Zürich: Geographisches Institut, Eidgenössische Technische Hochschule Zürich, Pp. 13– 23.*

Smith, D.M., Screen J.A., Deser C., et al (2019) The Polar Amplification Model Intercomparison Project (PAMIP) contribution to CMIP6: investigating the causes and consequences of polar amplification. Geosci Model Dev 12:1139–1164. doi: 10.5194/gmd-12-1139-2019.

Tucker, S. O., Kendon, E. J., Bellouin, N., Buonomo, E., Johnson, B., Murphy, J. M. (2021). *Evaluation of a new 12km regional perturbed parameter ensemble over Europe (submitted)*.

Walters, D., Baran, A., Boutle, I., Brooks, M., Earnshaw, P., Edwards, J., Furtado, K., Hill, P., Lock, A., Manners, J., Morcrette, C., Mulcahy, J., Sanchez, C., Smith, C., Stratton, R., Tennant, W., Tomassini, L., Van Weverberg, K., Vosper, S., … Zerroukat, M. (2017). The Met Office Unified Model Global Atmosphere 7.0/7.1 and JULES Global Land 7.0 configurations. *Geoscientific Model Development Discussions*, 1–78. https://doi.org/10.5194/gmd-2017-291.

Wang, F., Cheruy F., Vuichard N., Hourdin, F., 2016 The impact of heat roughness length on surface meteorology in IPSL - CM model , AMA (Ateliers de Modélisation Atmosphérique), Toulouse, 18-22 Jan. 2016.